Emission from the relativistic jets of AGN

Maria Petropoulou
Purdue University

Athens, July 14

mpetropo@purdue.edu

Hel.a.S
HELLENIC ASTRONOMICAL SOCIETY

Outline

- Active Galactic Nuclei (AGN)
- Evidence for relativistic motion in blazar jets
- Radiation physics of relativistic outflows
  - Lorentz transformations
  - Radiative processes:
    * synchrotron radiation
    * Inverse Compton scattering
- Models for blazar emission

Bibliography: Lecture notes on HEA by A. Mastichiadis & N. Vlahakis (UoA); Rybicki & Lightman (1979+); Dermer & Menon (2009)

Active Galactic Nuclei

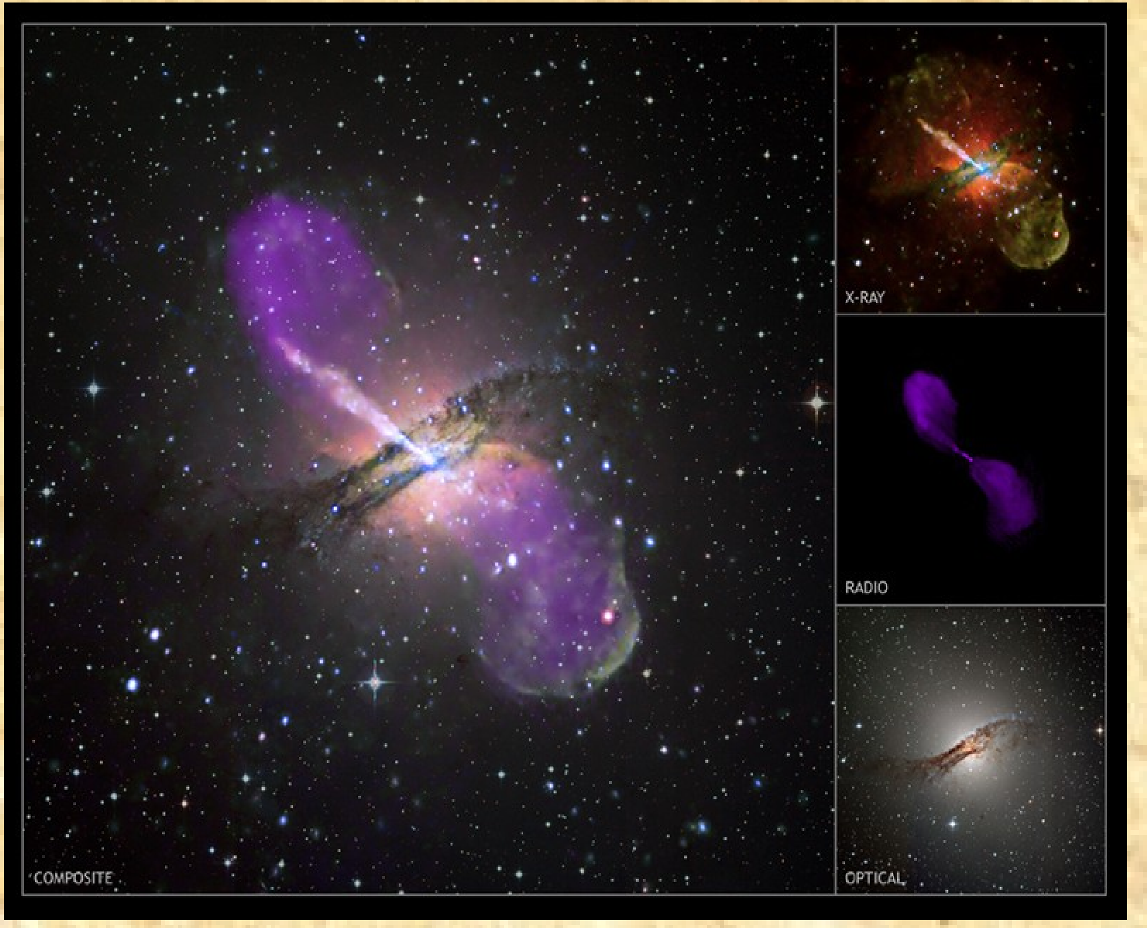

X-ray - NASA, CXC, R.Kraft (CfA), et al.; Radio - NSF, VLA, M.Hardcastle (U Hertfordshire) et al.; Optical - ESO, M.Rejkuba (ESO-Garching) et al.

-1/4-

Characteristics of AGN

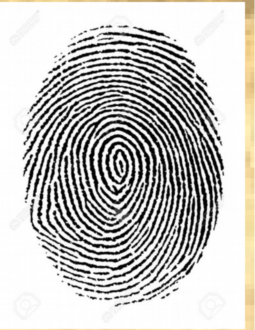

- Central nucleus outshines the rest of the galaxy

  How would the spectrum of a normal galaxy look like compared to that of an AGN ? (qualitatively)

- High luminosity (> 10^{42} erg/s)
- Emission extends over many orders of magnitude in energy (e.g. radio to keV/MeV or GeV/TeV)
- Flux variability
- Radio emission from certain AGN

  – relativistic jets, superluminal motion etc.

AGN vs. Normal galaxy emission

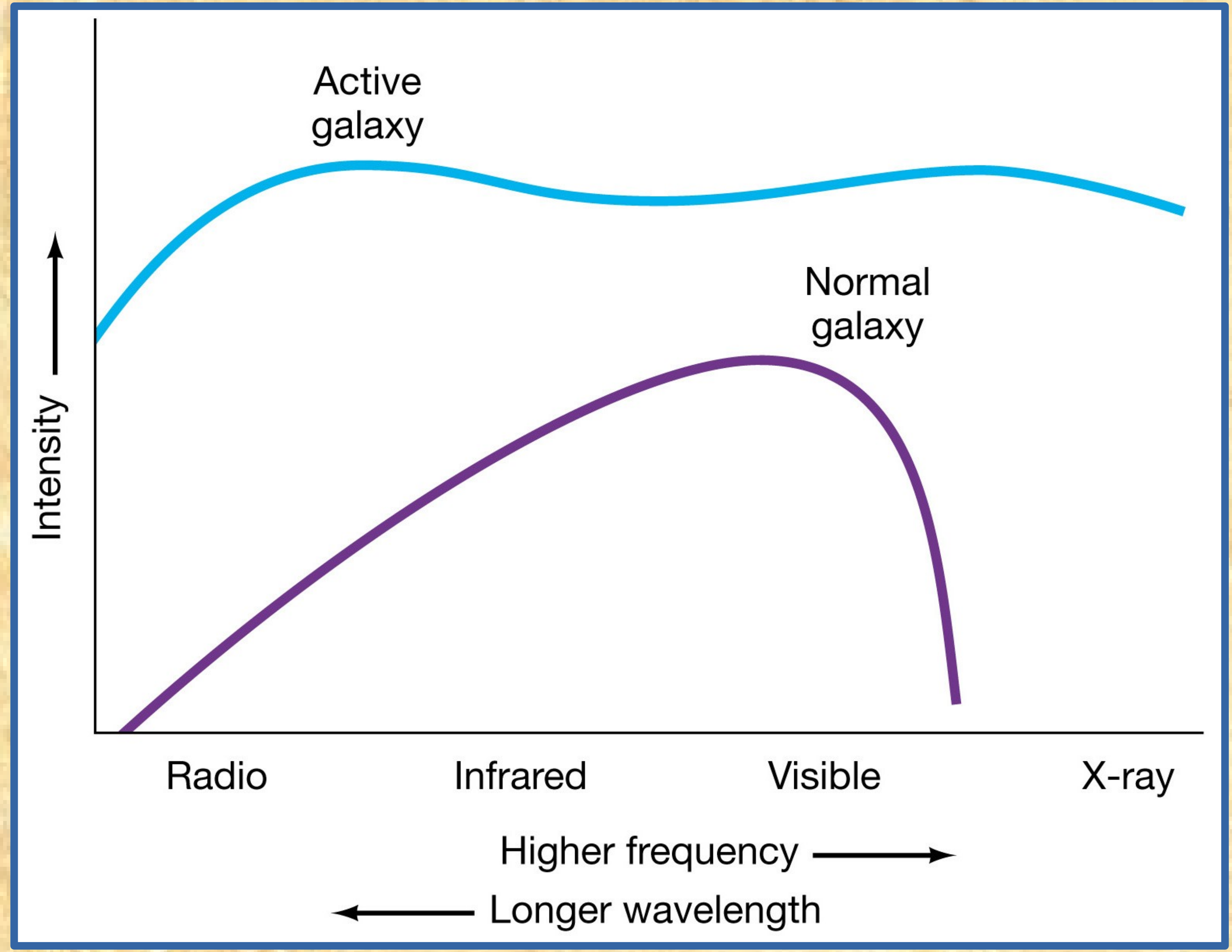

Taxonomy of AGN

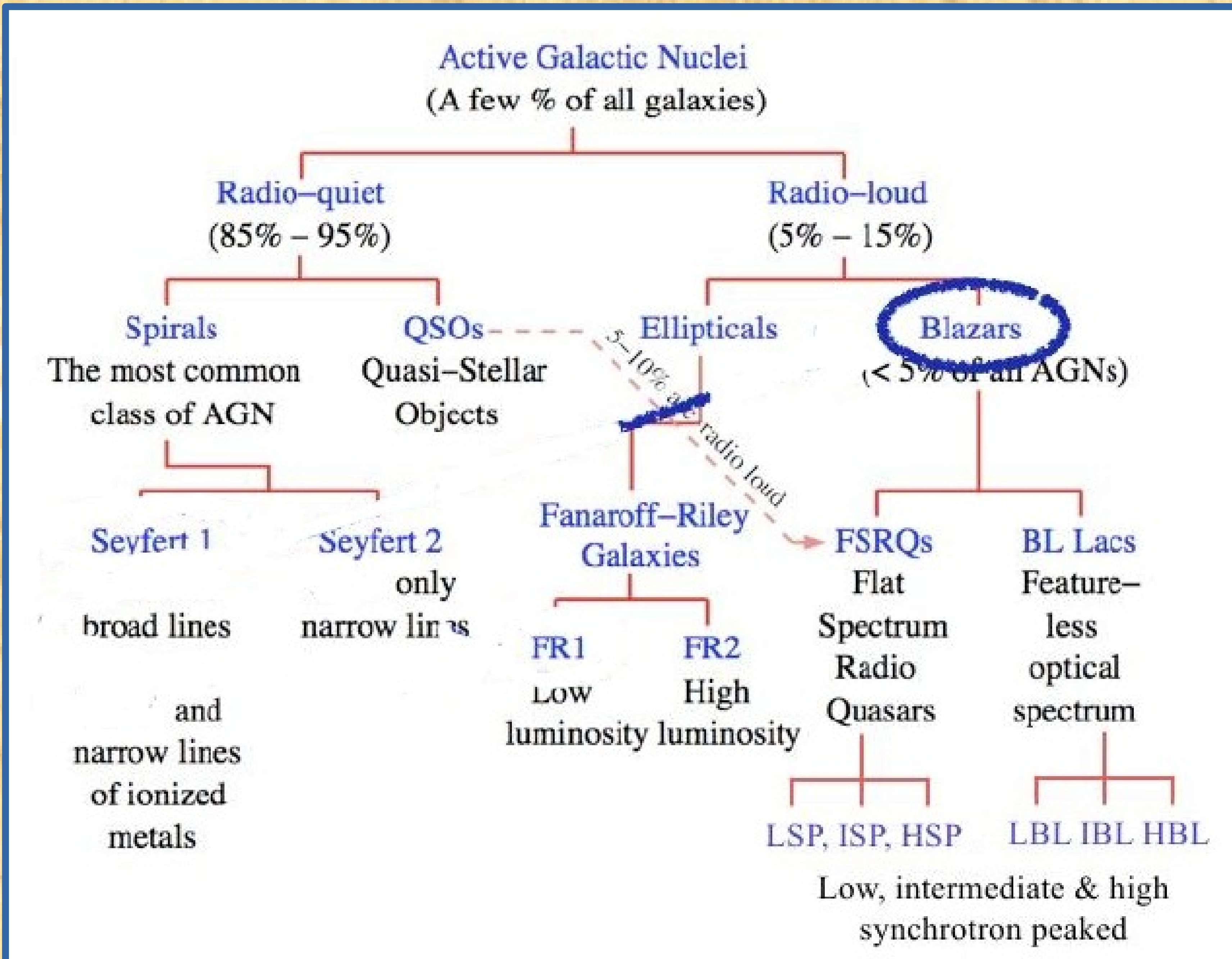

Taxonomy of AGN

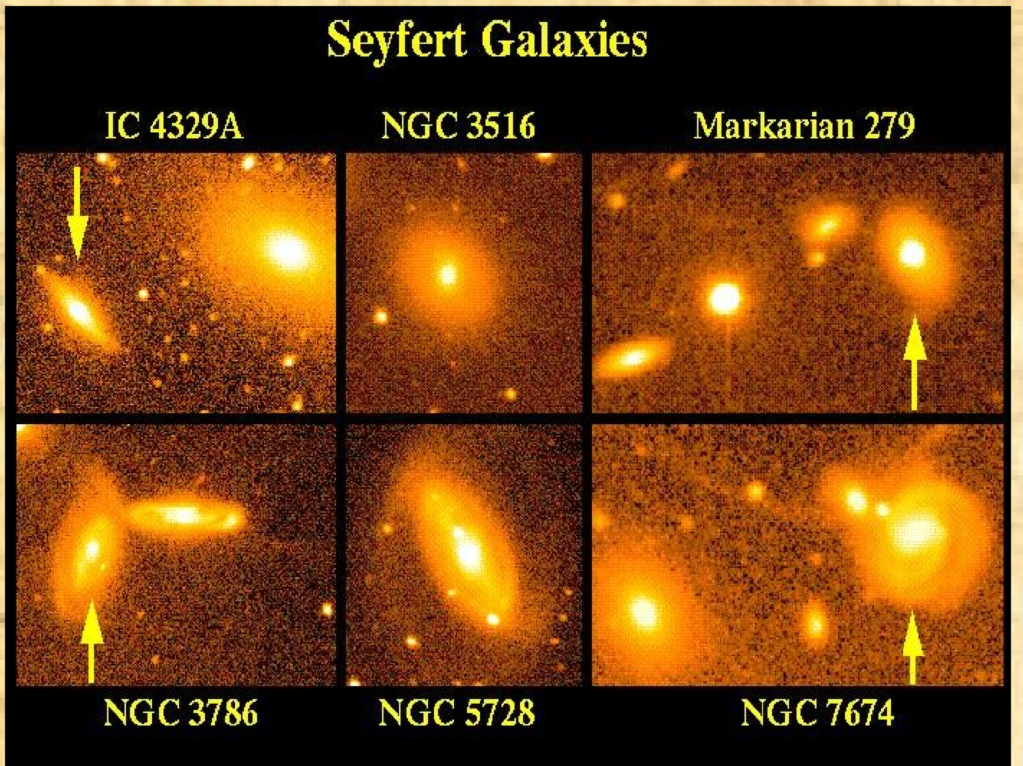

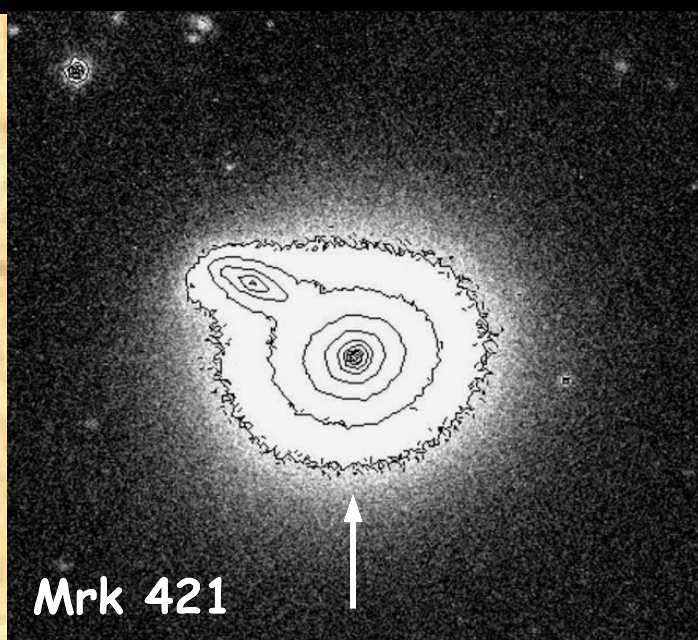

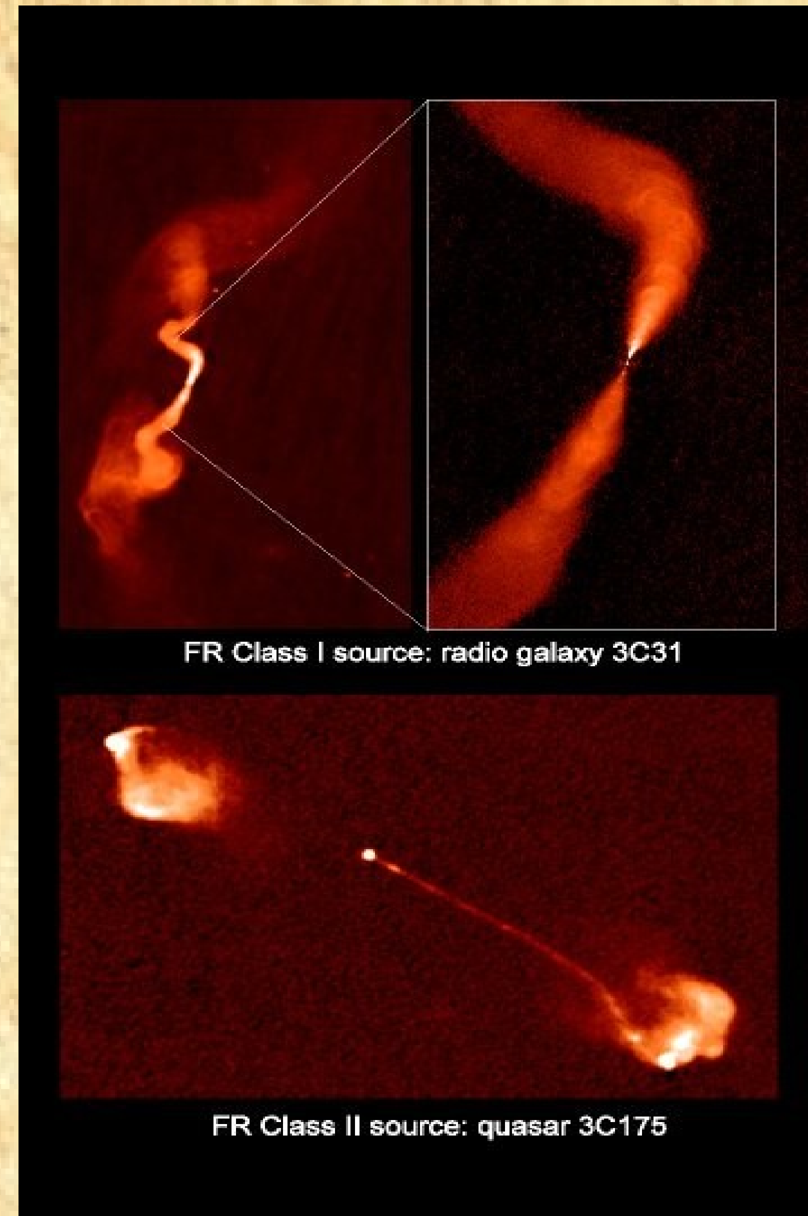

FR Class I source: radio galaxy 3C31

FR Class II source: quasar 3C175

Optical spectra of AGN

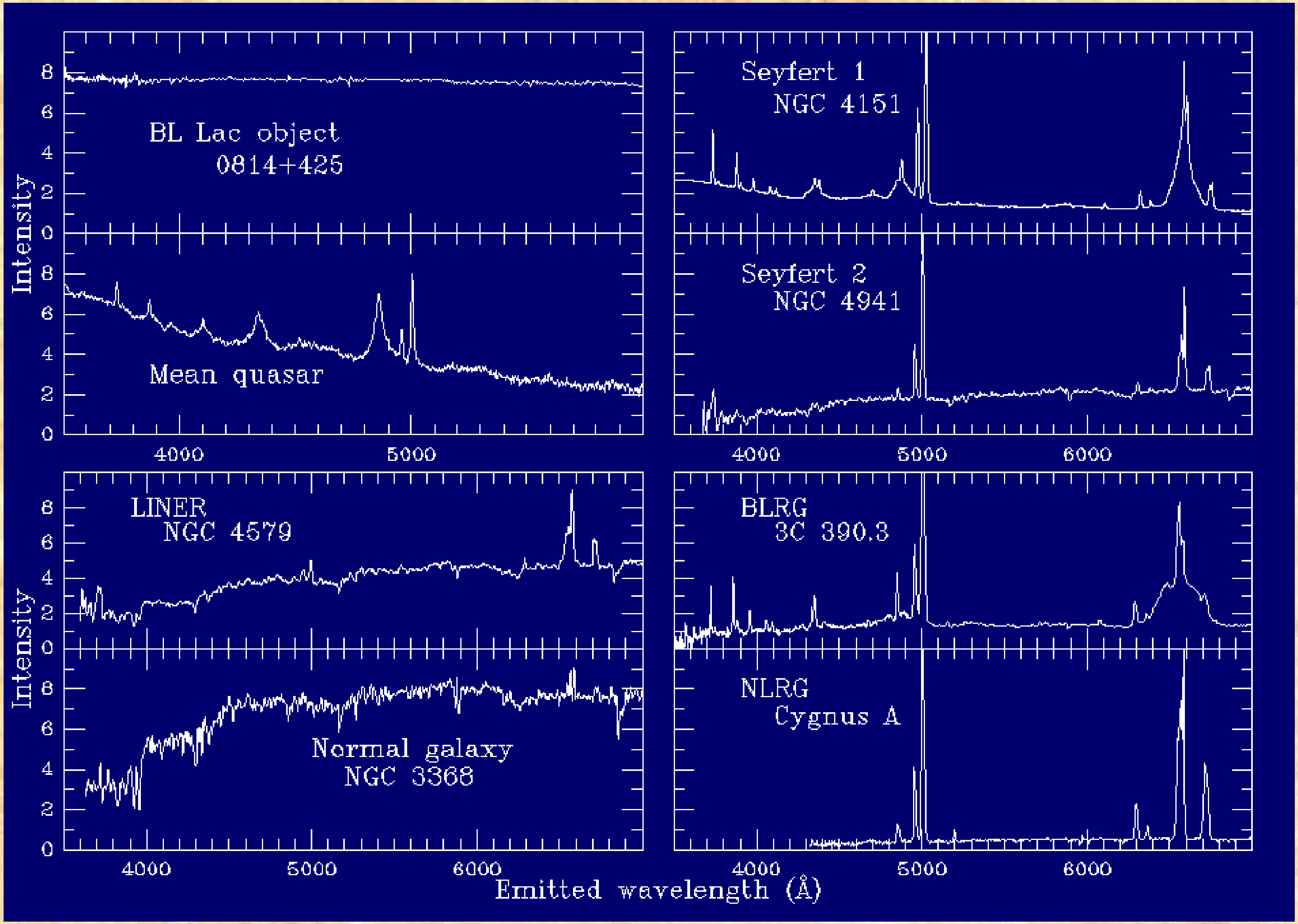

Unification of AGN

First unification attempts in the 70's

ON THE UNITY OF ACTIVITY IN GALAXIES

M. ROWAN-ROBINSON
Dept. of Applied Mathematics, Queen Mary College, Mile End Rd., London E1

Received 1976 May 20; revised 1976 October 26

ABSTRACT

A scheme is presented which unites quasars, radio galaxies, N galaxies, and Seyfert galaxies into a single picture of activity in galaxies. Probability functions are given for optical and radio cores, and extended radio sources (in the case of ellipticals), for both spirals and ellipticals. Activity occurs in galaxies of all luminosities, but the strength of it is made proportional to galaxy luminosity. It is assumed that there is dust surrounding the optical cores, to explain the strong infrared emission in Seyferts.

Quasars may, in this picture, occur in both spirals and ellipticals, and in fact most optically selected QSOs are predicted to be in spirals.

Subject headings: galaxies: nuclei — galaxies: Seyfert — galaxies: structure — quasars — radio sources: general

THE ASTROPHYSICAL JOURNAL, 213:635–647, 1977 May 1

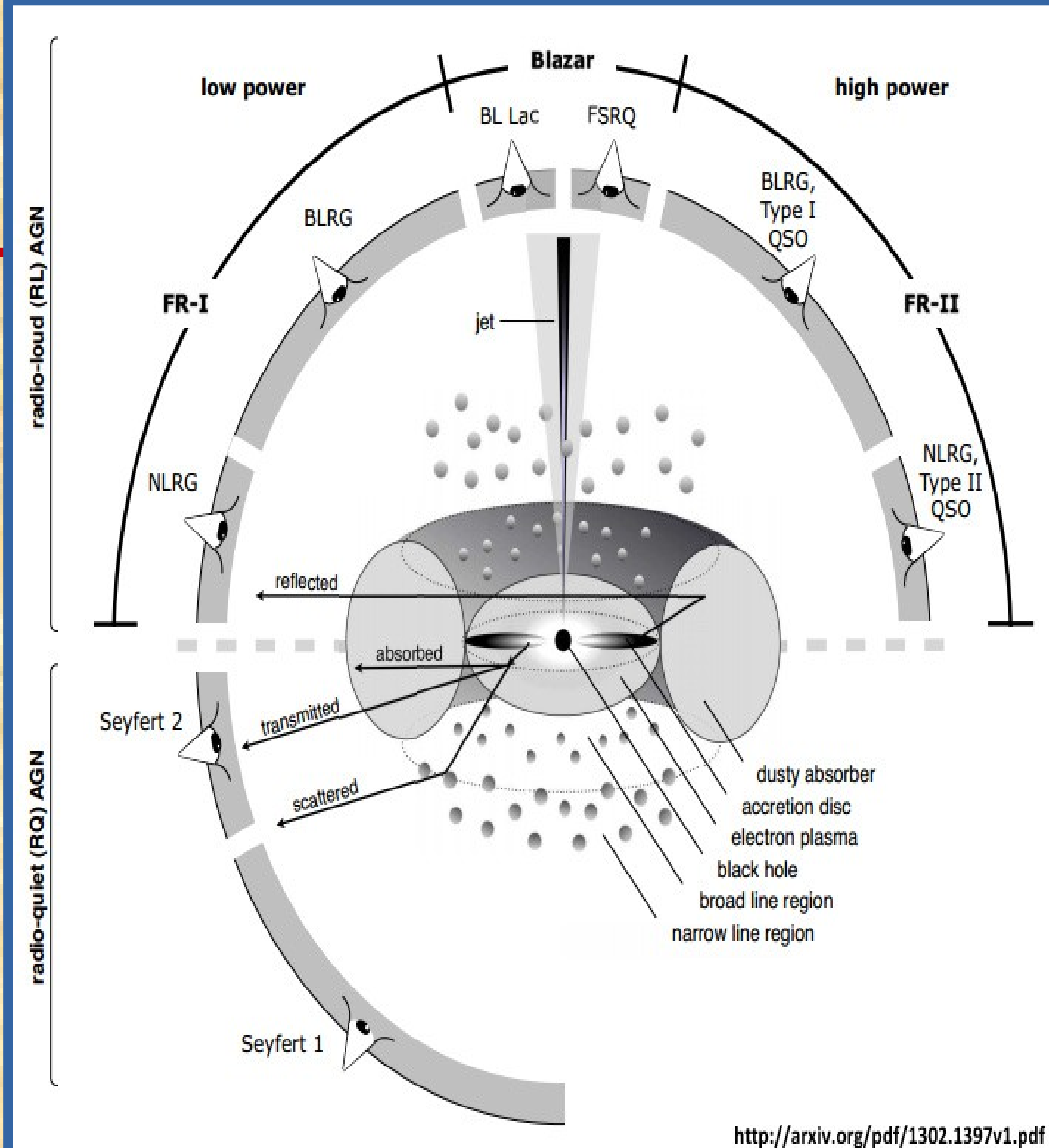

Unification scheme of Urry & Padovani (1990)

Blazars vs. Seyferts

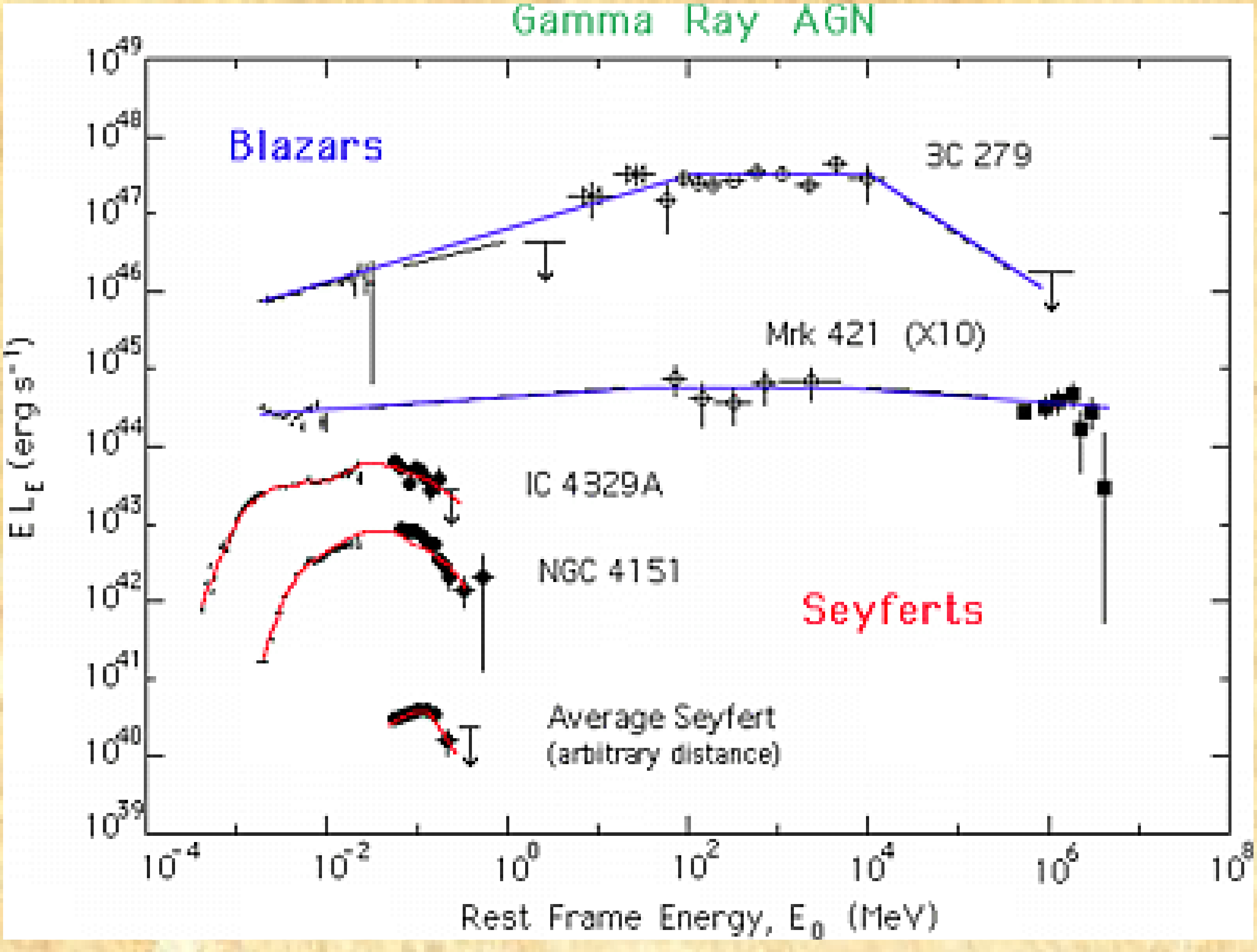

Seyfert spectra extend up to ~keV energies; lower luminosity

Blazar spectra extend up to GeV-TeV energies; higher luminosity

Evidence for relativistic motion

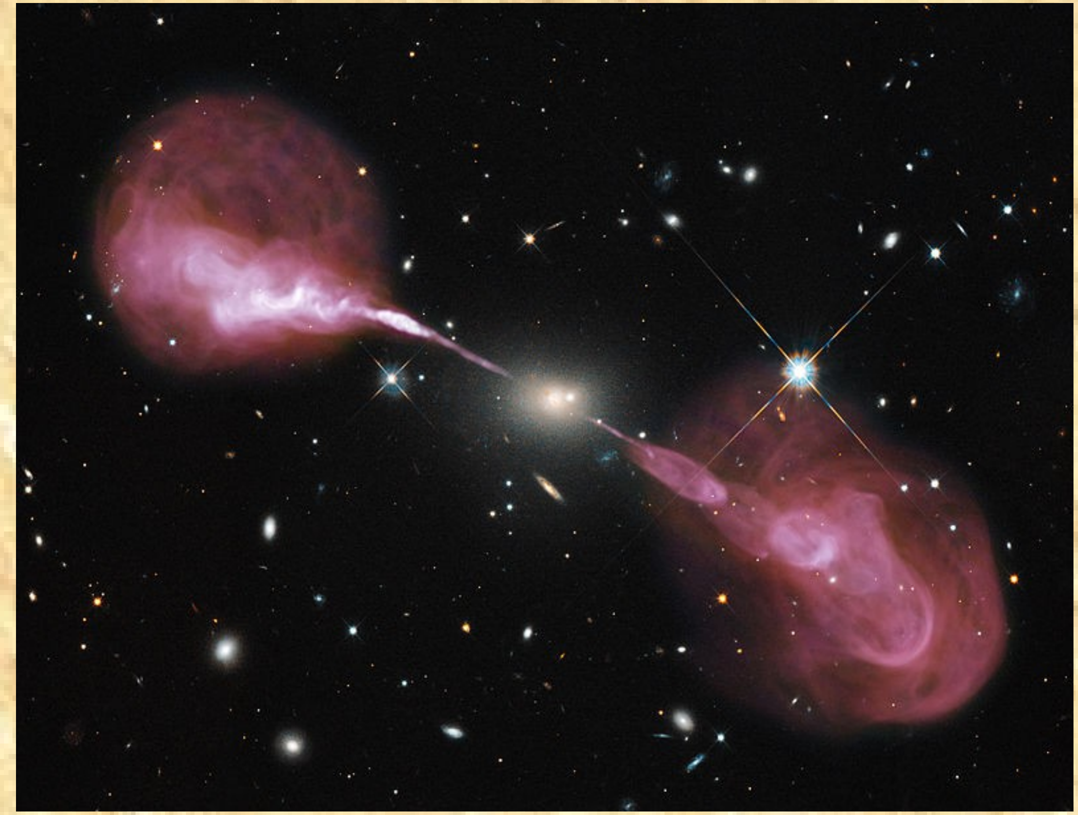

NASA, ESA, S. Baum and C. O'Dea (RIT), R. Perley and W. Cotton (NRAO/AUI/NSF), and the Hubble Heritage Team (STScI/AURA) - http://www.spacetelescope.org/images/opo1247a/

a) Superluminal motion

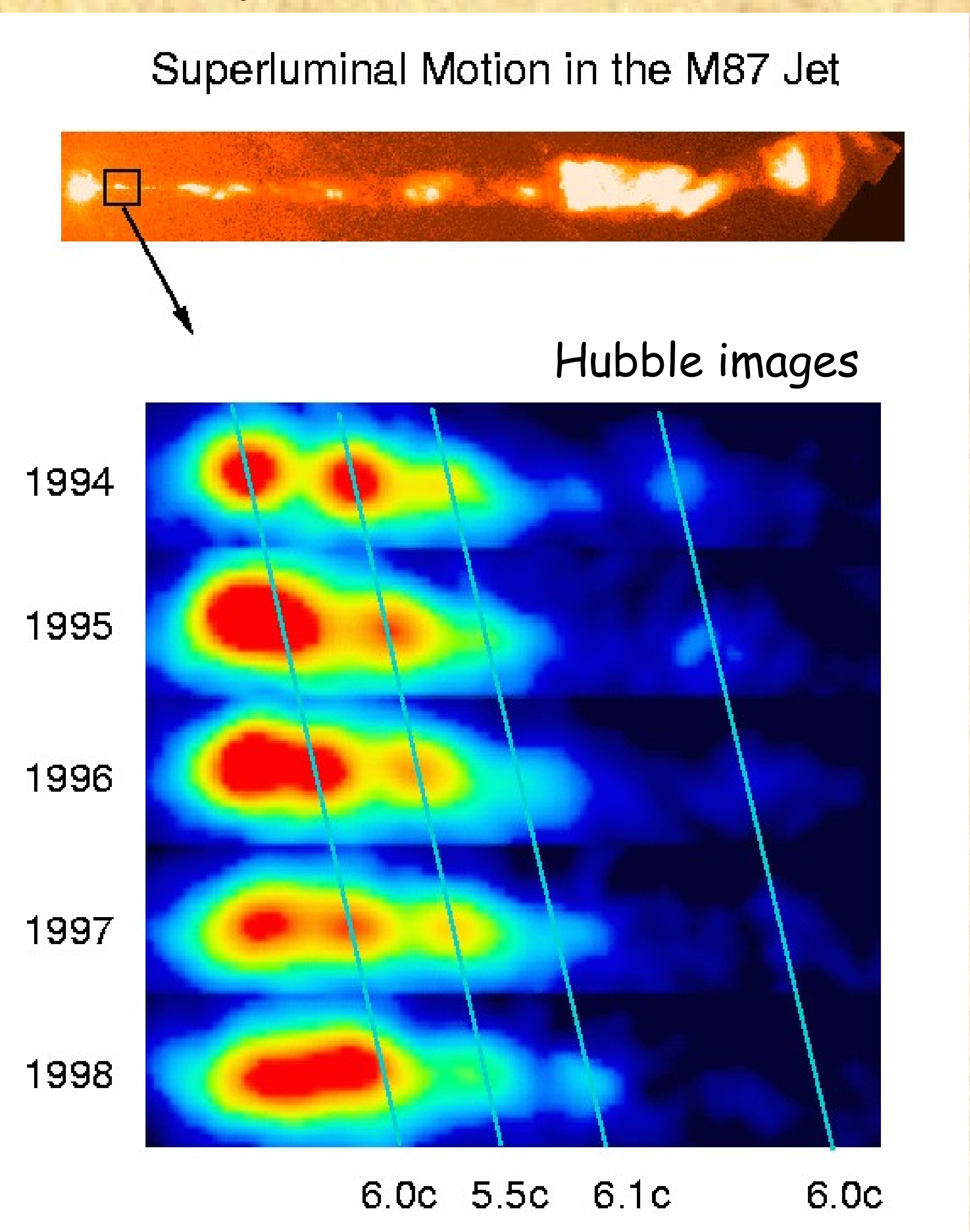

- The velocity of the knots is larger than the speed of light !
- This is called apparent velocity.
- It is the result of the relativistic motion of the knots and of the geometry.

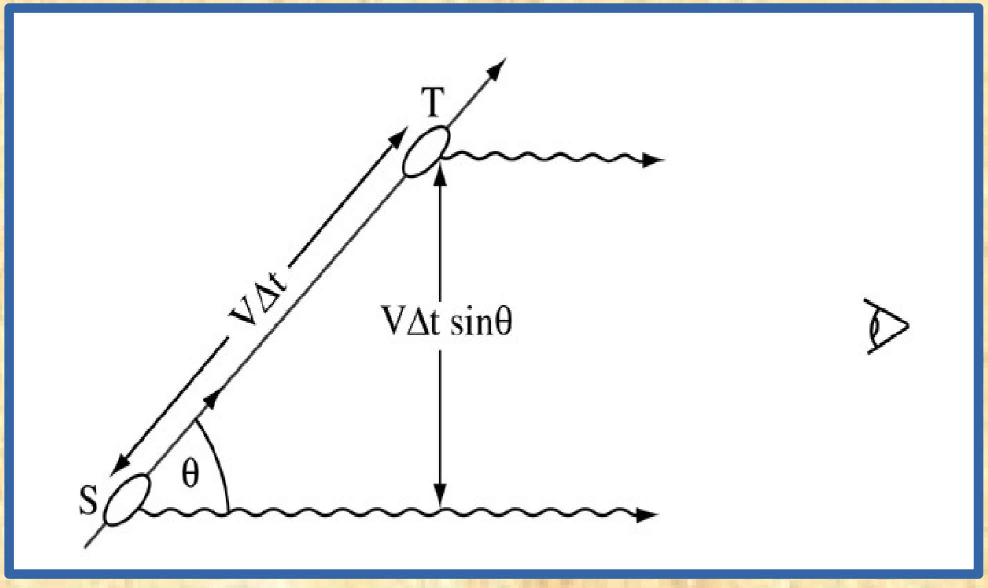

http://www.physics.purdue.edu/astro/MOJAVE/movies.html

a) Superluminal motion

Apparent velocity:

$$\beta_{app} = \frac{\beta \sin\theta}{1 - \beta \cos\theta}$$

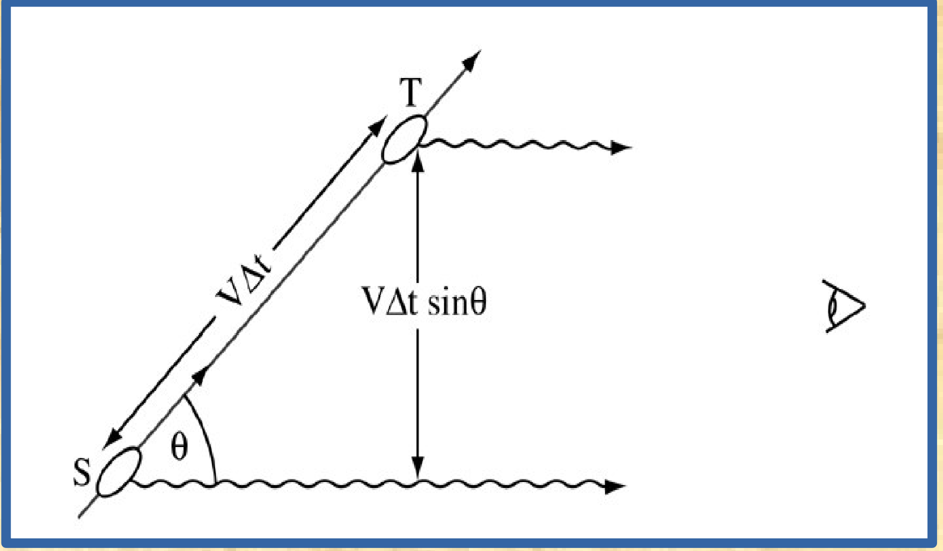

- Can we observe superluminal motion for all velocities of the knots?

- What are the conditions for superluminal motion?

- What is the angle that maximizes the apparent velocity?

- The maximum apparent velocity depends upon what?

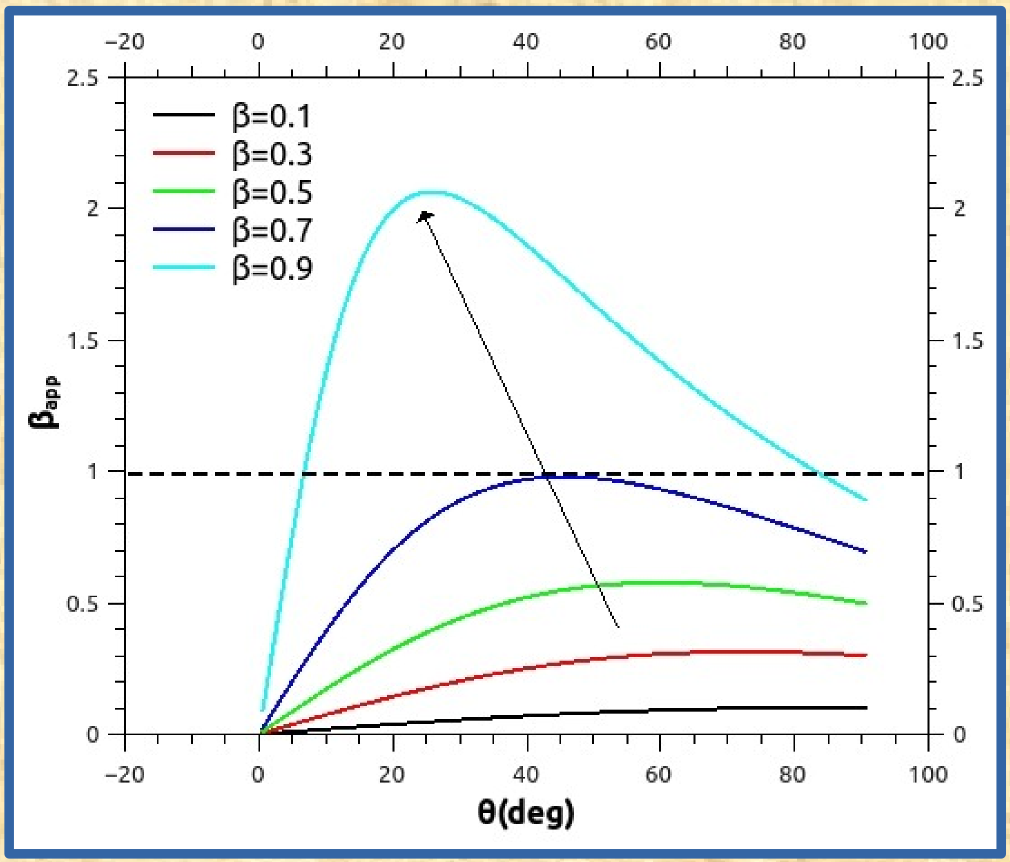

b) γγ opacity

Can the γ-rays escape from a compact source?

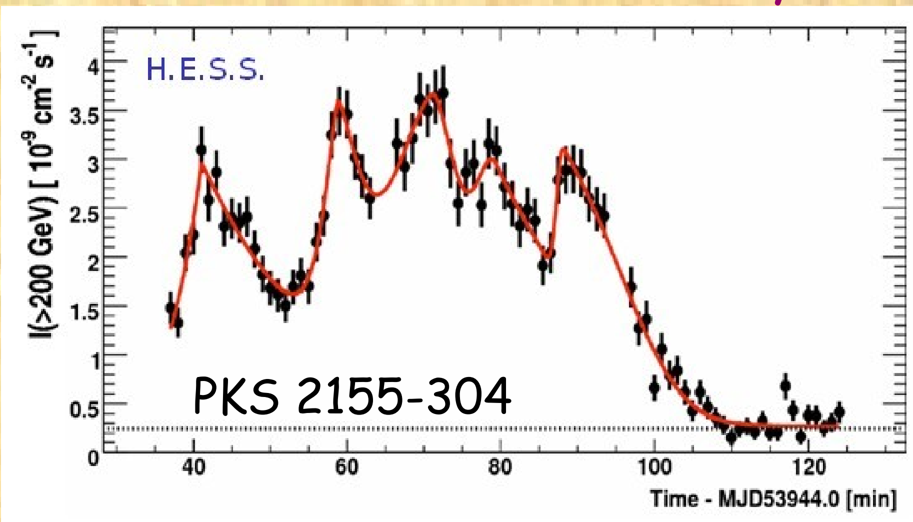

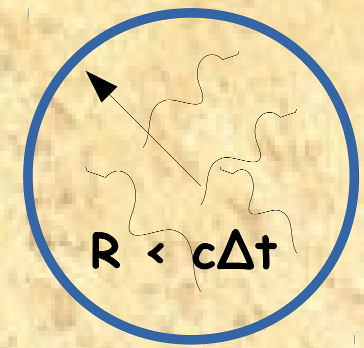

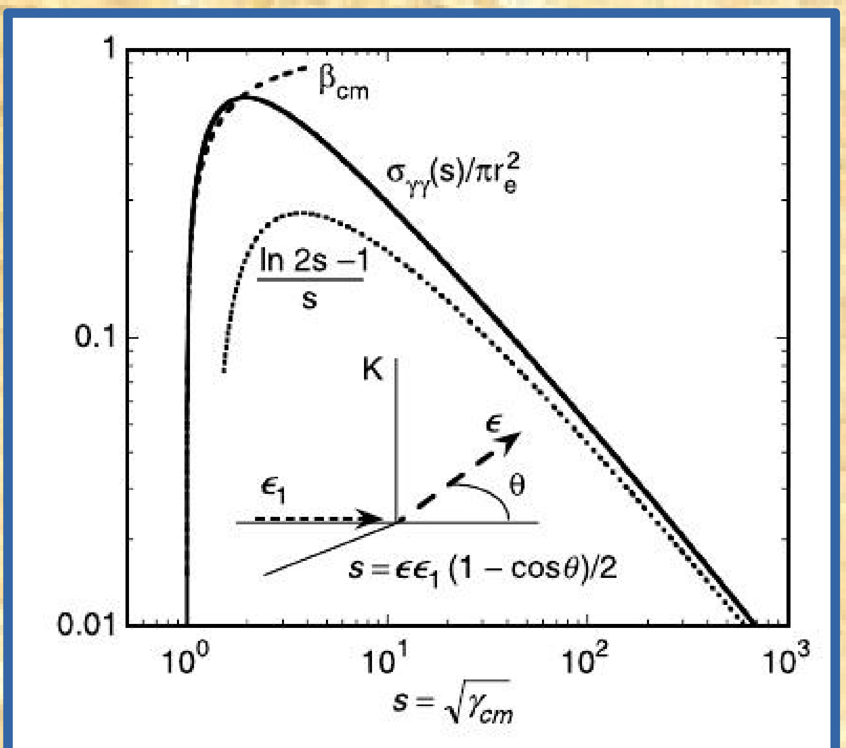

$$\sigma_{\gamma\gamma}(s) = \frac{1}{2}\pi r_e^2 (1-\beta_{\rm cm}^2)\left[(3-\beta_{\rm cm}^4)\ln\left(\frac{1+\beta_{\rm cm}}{1-\beta_{\rm cm}}\right) - 2\beta_{\rm cm}(2-\beta_{\rm cm}^2)\right]$$

$$\sigma_{\gamma\gamma}(\epsilon\epsilon_1) \cong \frac{2}{3}\sigma_{\rm T}\,\delta(\epsilon\epsilon_1 - 2)$$

b) γγ opacity

Can the γ-rays escape from a compact source?

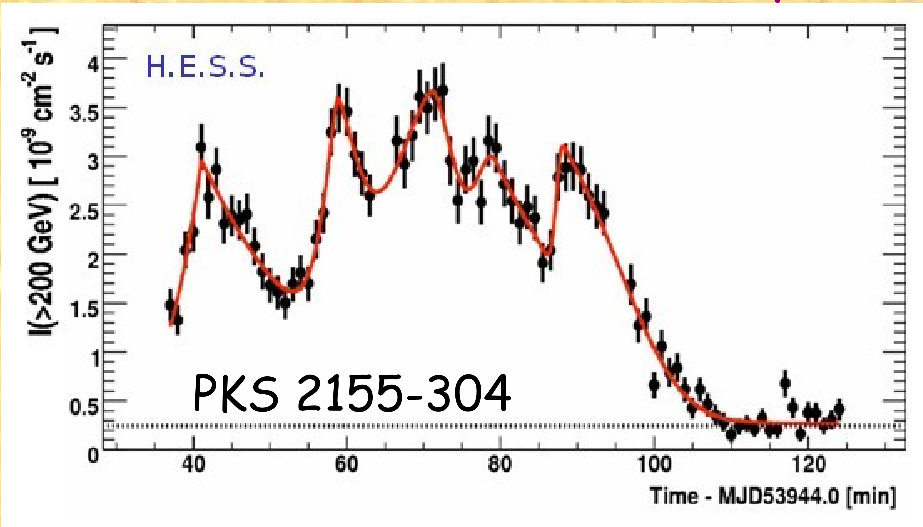

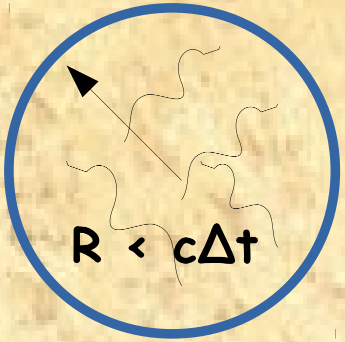

$$\sigma_{\gamma\gamma}(\epsilon\epsilon_1) \cong \frac{2}{3}\sigma_T\,\delta(\epsilon\epsilon_1 - 2)$$

$$n(\varepsilon) \approx \frac{L}{4\pi c R^2 \varepsilon_0}\delta(\varepsilon - \varepsilon_0)$$

$$\tau_{\gamma\gamma} \approx R \int d\varepsilon\, n(\varepsilon)\,\sigma(\varepsilon\varepsilon_1)$$

$$\tau_{\gamma\gamma} \approx 300\,\frac{L_{48\,erg/s}}{\Delta t_{1d}}$$

PROBLEM: The source should not be observed in γ-rays!!

SOLUTION: The source moves relativistically.

Radiation physics of relativistic outflows

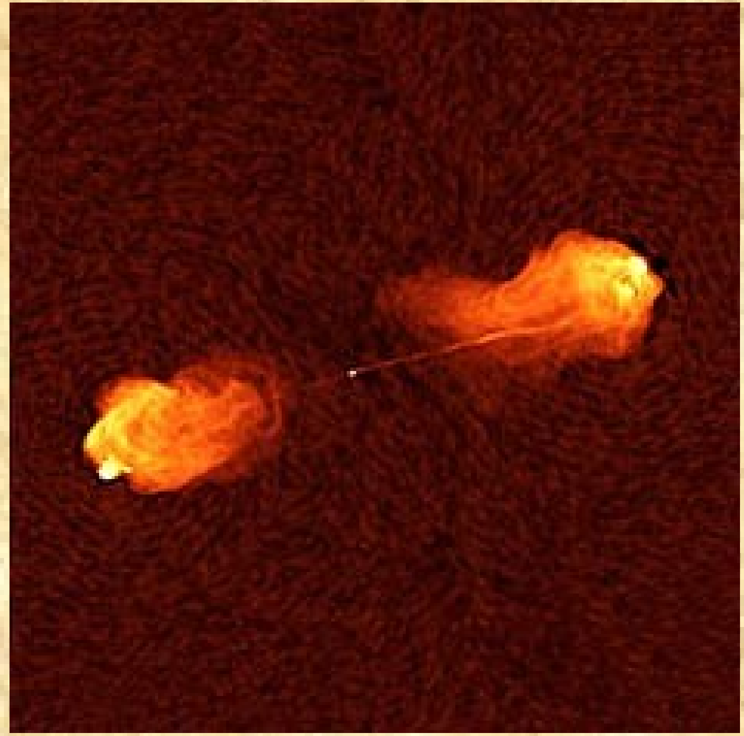

http://hubblesite.org/

-3/4-

Invariant quantities

- Four-volume: $dV = dt\, d\vec{x}$
- Phase-volume: $d\mathbf{V} = d\vec{x}\, d\vec{p}$

$$\frac{dN}{d\mathcal{V}} = \frac{1}{p^2}\,\frac{dN}{dV\,dp\,d\Omega} \Rightarrow \frac{1}{\epsilon^2}\,\frac{dN}{dV\,d\epsilon\,d\Omega} = \frac{1}{m_e c^2 \epsilon^3}\,\frac{d\mathcal{E}}{dV\,d\epsilon\,d\Omega} \equiv \frac{1}{\epsilon^3}\,\frac{u(\epsilon,\Omega)}{m_e c^2}$$

$$E\,\frac{dN}{d^3\vec{x}\,dt\,d^3\vec{p}} = \frac{1}{\epsilon^2}\,\frac{d\mathcal{E}}{dV\,dt\,d\epsilon\,d\Omega} \equiv \frac{1}{\epsilon^2}\,j(\epsilon,\Omega)$$

$$\frac{dN}{\epsilon\,d\epsilon\,d\Omega} = \frac{N(\epsilon,\Omega)}{\epsilon}$$

Derive the last equality.
(Hint: You should first prove the invariance of $d\vec{p}/\varepsilon$)

Animated Examples of the Acoustic Doppler Effect

In these animations a soldier is repeatedly buzzed by an annoying UAV. Each animation lasts 8 seconds, with the following cases being demonstrated:

1. Constant speed (100m/s) horizontal flight
   a. passing 4m overhead
   b. passing 125m overhead
   c. passing 250m overhead
2. Constant height (100m) horizontal flight
   a. passing at Mach 0.25
   b. passing at Mach 0.5
   c. passing at Mach 1.0 ;-)
3. Unsteady motion
   a. accelerating at $20m/s^2$ from stand-still
   b. surging forwards
   c. wavy flight

Please note that the sprites and sound wavelength are NOT drawn to scale. The domain actually represents a 0.8 x 0.45km region. The equation for generating Doppler shifted signals is given at the end….

Transformations-1

- Photon/Particle energy: $$\varepsilon' = \Gamma\varepsilon(1-\beta\mu) = \frac{\varepsilon}{\delta_D}$$
- Angle: $$\mu' = \frac{\mu-\beta}{1-\beta\mu}$$
- Solid angle: $$d\Omega' = \frac{d\Omega}{\Gamma^2(1-\beta\mu)^2} = d\Omega\,\delta_D^2$$
- Time interval of emission: $$dt = \Gamma\, dt'$$
- Time interval of received radiation: $$dt = \Gamma(1-\beta\mu)\,dt' = \frac{dt'}{\delta_D}$$

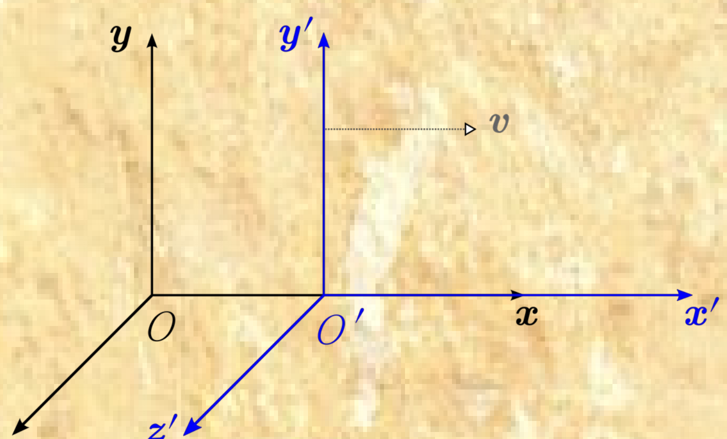

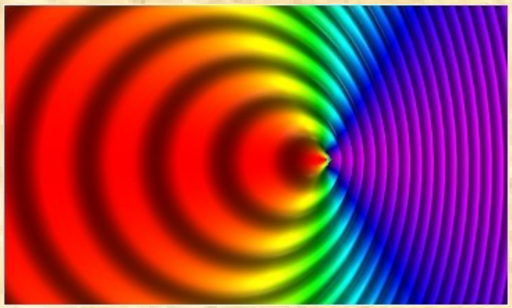

Transformations-2

- Total Energy (in particles or photons): E=Γ*E'

  Show this relation for an isotropic and monochromatic photon field in the comoving frame of the source.

- Differential Photon energy density:

$$u'(\epsilon', \Omega') = \frac{u(\epsilon, \Omega)}{\Gamma^3(1+\beta\mu')^3}$$

What is the energy density of an external isotropic and monochromatic photon field in the rest frame of the source?
(e.g. Broad Line Region - BLR)

$$u'_0 = \Gamma^2 u_0 \left(1+\frac{\beta^2}{3}\right)$$

What is the energy density of a monochromatic photon field that lies “behind” the source as seen in the comoving frame?
(e.g. accretion disk)

$$u'_0 = \frac{u_0}{\Gamma^2 (1+\beta)^2}$$

Observed Fluxes

$$d[\varepsilon F(\varepsilon,\Omega)]=\delta_D^4\frac{\varepsilon' j'(\varepsilon',\Omega')dV'}{d_L^2}=\delta_D^4\frac{\varepsilon' L'(\varepsilon',\Omega')}{d_L^2}$$

REVISION: What is the γγ opacity of a γ-ray emitting source that moves relativistically? – It is smaller by a factor of Doppler^3!

- Total emitted power:

$$L_{em}=\int d\Omega\frac{L_{iso}}{4\pi}=\int d\Omega\frac{\delta_D^4 L'}{4\pi}\approx\Gamma^2 L'$$

Synchrotron Radiation - 1

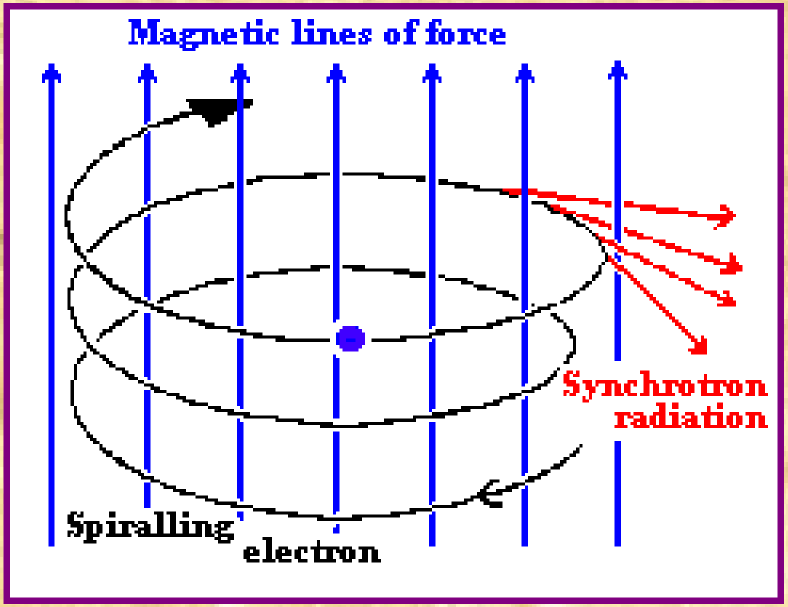

- Radiation produced by relativistic electrons ($E=m\gamma c^2 \gg mc^2$) due to their accelerated motion in the magnetic field B.
- No acceleration // to B → cyclic motion + constant velocity // to B.
- Acceleration: $a=\omega_B v_{perp}=\omega_B v \sin a$
- Gyration frequency: $\omega_B=qB/m\gamma c$
- Larmor formula: $$P=\frac{2q^4}{3c^3}\gamma^4(a_\perp^2+\gamma^2 a_\parallel^2)$$

- Synchrotron Power:

$$P=\frac{1}{4\pi}\sigma_T c B^2 \beta^2 \gamma^2 (\sin a)^2$$

- Synchrotron averaged power:

$$P=\frac{1}{6\pi}\sigma_T c B^2 \beta^2 \gamma^2$$

- Energy loss time scale:

$$t_{syn}=\frac{E}{P_{syn}} \propto B^{-2}\gamma^{-1}$$

Synchrotron Radiation - 2

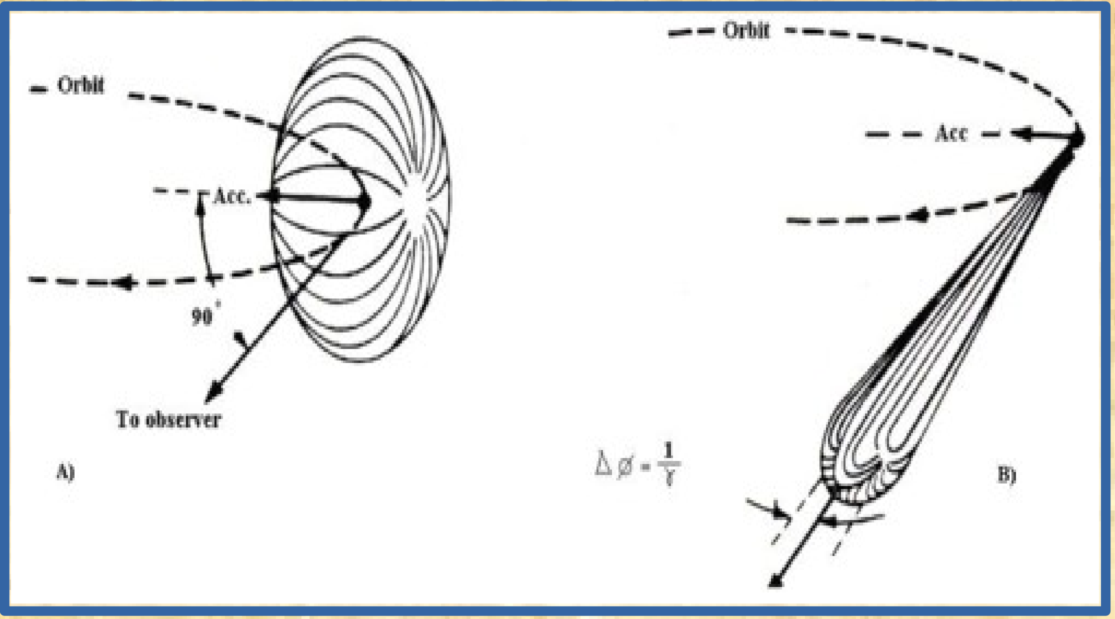

The radiation is beamed within an angle ~1/γ.

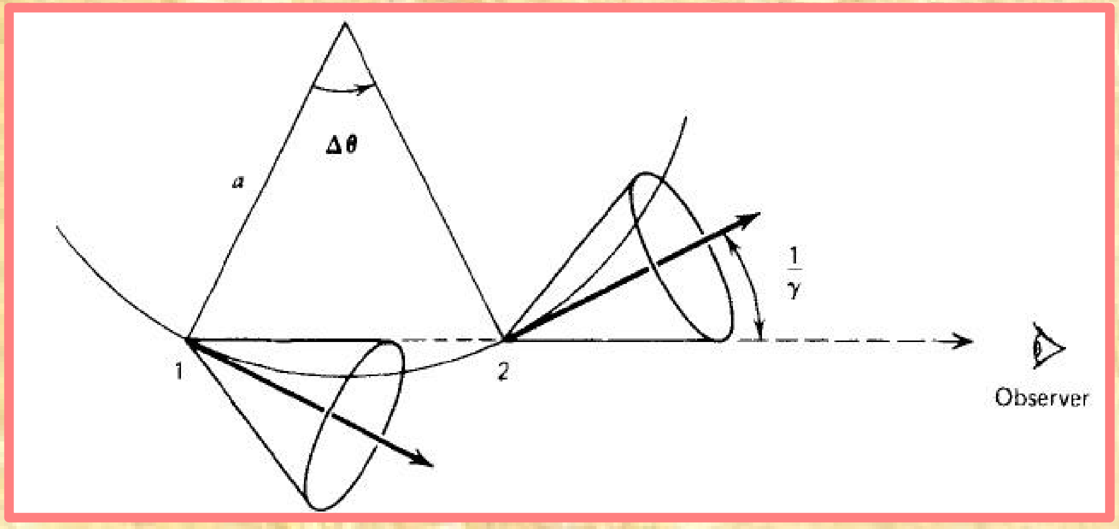

Duration of a pulse seen by the observer:

$$\Delta t \approx \frac{1}{\gamma^3 \omega_B sina}$$

Characteristic frequency of emission:

$$\omega_c \approx \frac{1}{\Delta t} \approx \frac{3}{2} \gamma^3 \omega_B sina$$

Synchrotron Radiation - 3

Radiation from a single electron.

Emitted spectrum of synchrotron radiation:

$$P(\omega) = \frac{\sqrt{3}\, q^3 B \sin\alpha}{2\pi m c^2} F(x)$$

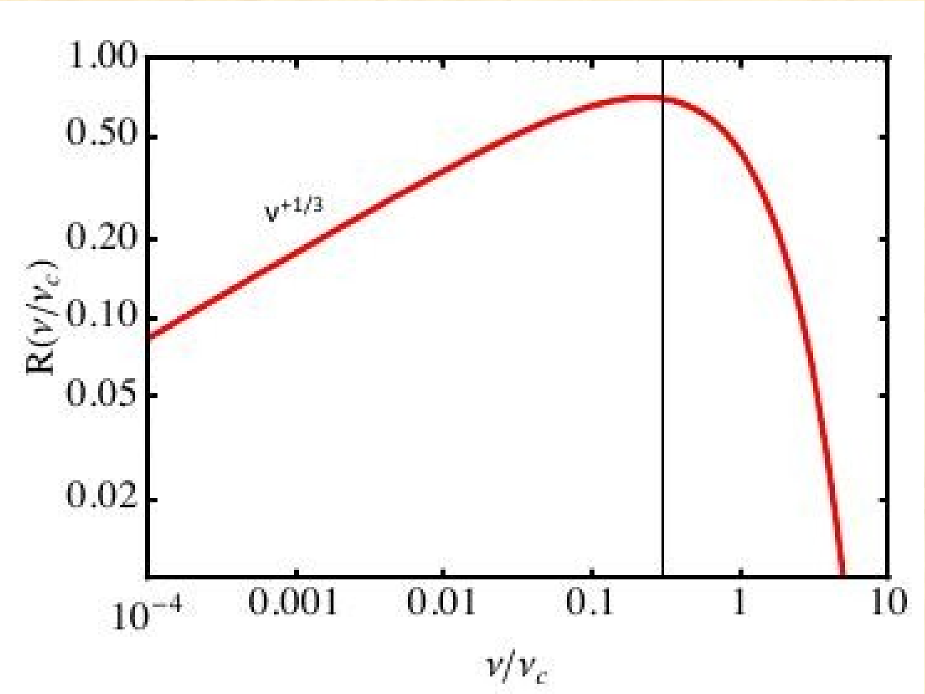

$x=\nu/\nu_c=\omega/\omega_c$

$$F(x) \equiv x \int_x^\infty K_{\frac{5}{3}}(\xi)\, d\xi,$$

Asymptotic Forms:

$$F(x) \sim \frac{4\pi}{\sqrt{3}\,\Gamma(\frac{1}{3})} \left(\frac{x}{2}\right)^{1/3}, \qquad x \ll 1,$$

$$F(x) \sim \left(\frac{\pi}{2}\right)^{1/2} e^{-x} x^{1/2}, \qquad x \gg 1.$$

Synchrotron Radiation - 4

Radiation from an electron distribution.

Qualitative description for the formation of a power law

$$N(\gamma) \propto \gamma^{-p}, \gamma_{min} \leqslant \gamma \leqslant \gamma_{max}$$

$$J(\nu) \propto \nu^{-(p-1)/2}, \nu_{min} \leqslant \nu \leqslant \nu_{max}$$

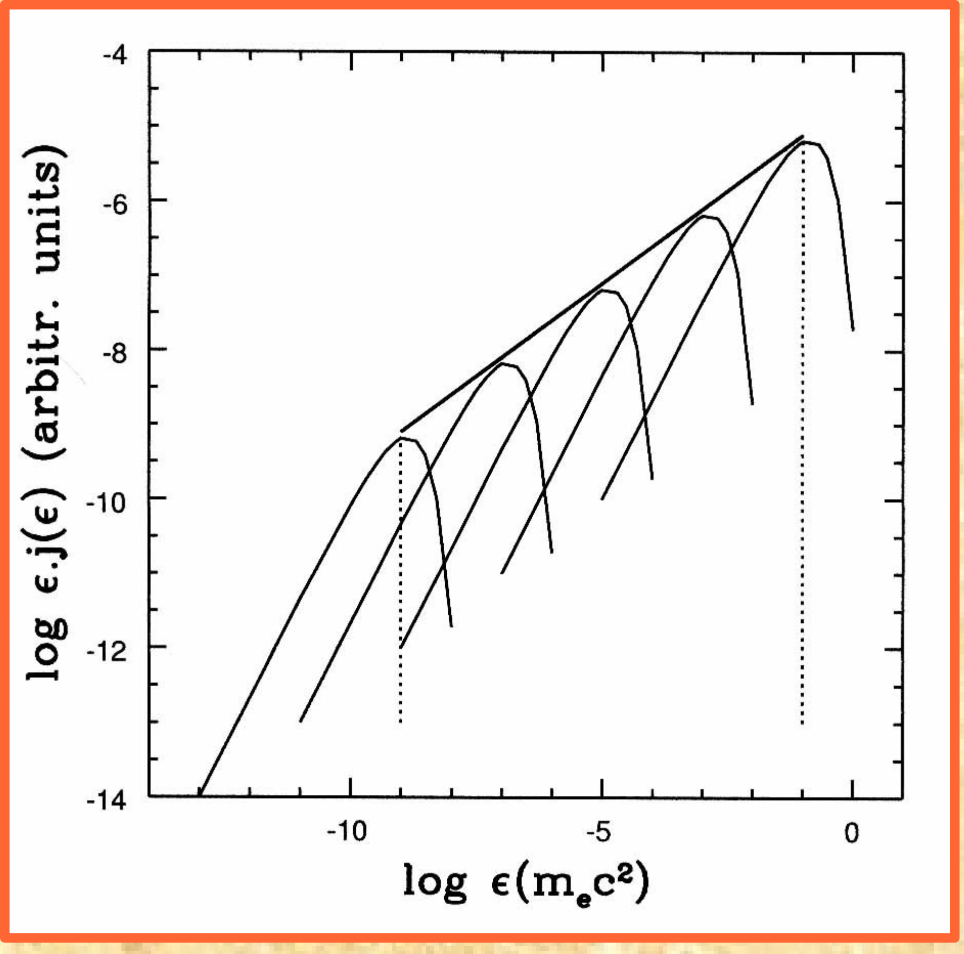

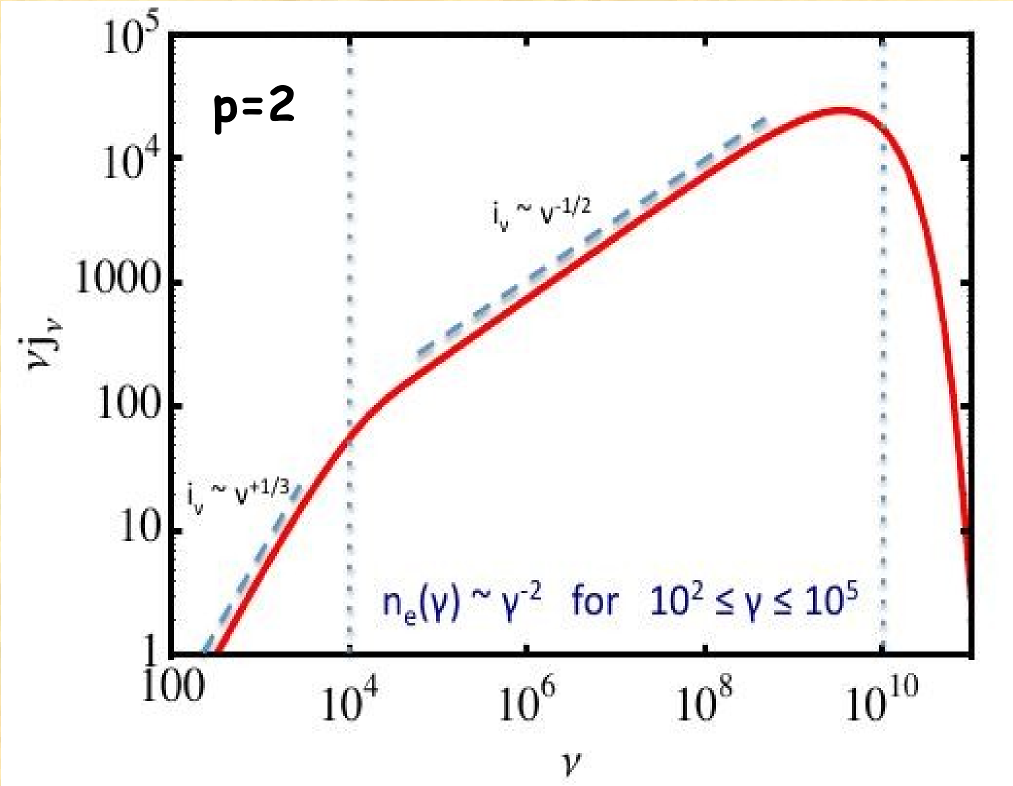

Synchrotron Radiation - 5

By approximating the synchrotron emissivity by a δ-function

$$j(\nu) = j_0 \delta(\nu - \nu_c)$$

derive the differential number density of synchrotron photons $n(\varepsilon)$ for a given electron distribution $n_e(\gamma)$.

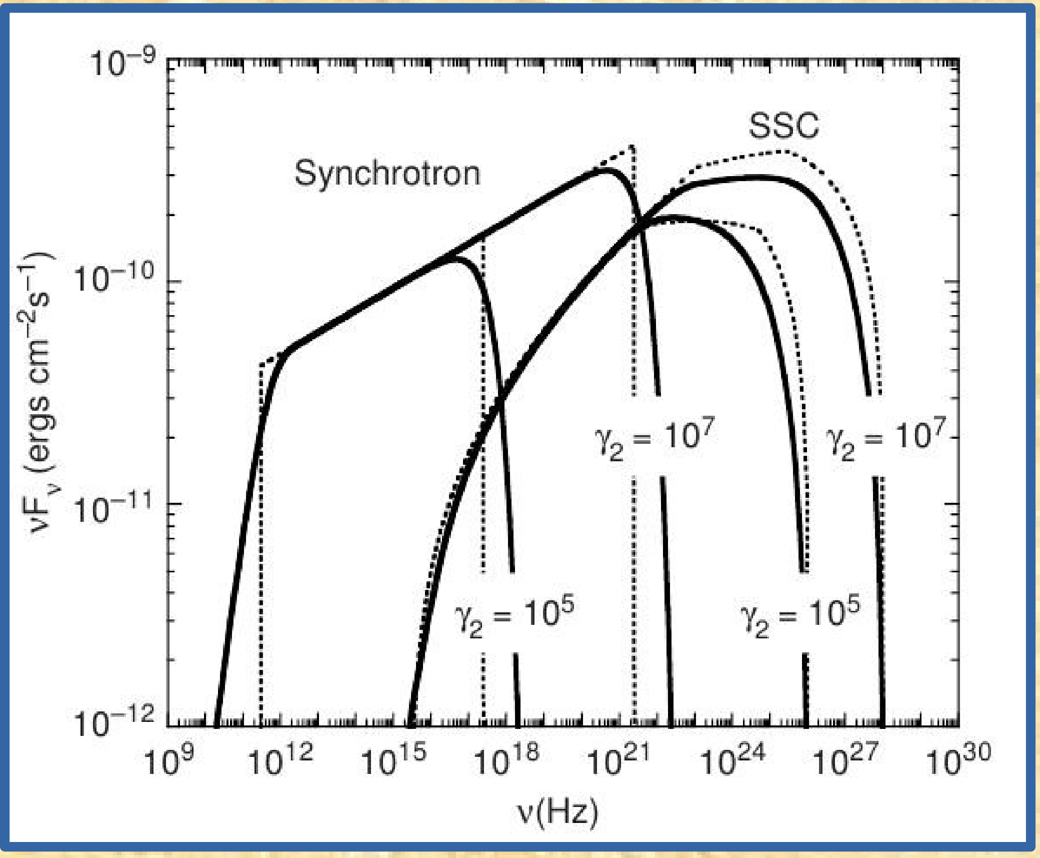

Comparison of the synchrotron spectra produced by a power-law electron distribution using the full expression (solid lines) and the δ-function approximation (dashed lines) (Credit: Dermer & Menon 2009).

Inverse Compton Scattering - 1

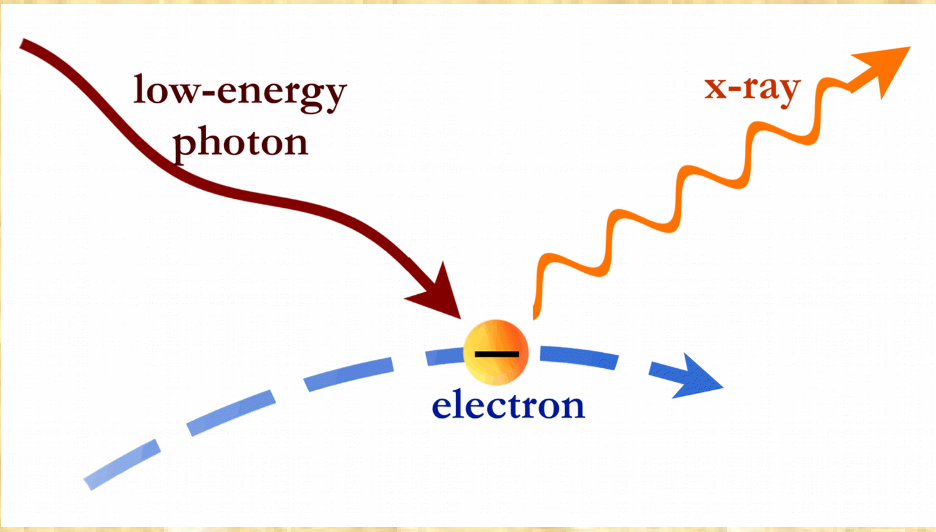

- If the kinetic energy of the electron is sufficiently high, energy may be transferred from the electron to the photon.

Electron Rest Frame (ERF)

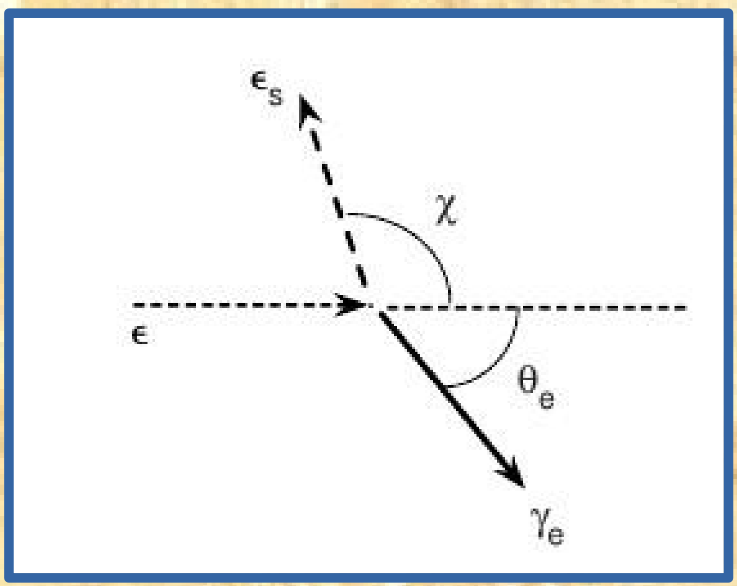

Energy of scattered photon

$$\varepsilon_1 = \frac{\varepsilon}{1+\varepsilon\left(1-\cos\chi\right)}$$

Using the conservation of energy and momenta derive the above relation.

- Thomson regime: $\varepsilon \ll 1$
- Max. scattered photon energy in Thomson: $4\gamma^2\varepsilon$
- Average scattered photon energy in Thomson: $\gamma^2\varepsilon$

Inverse Compton Scattering - 2

Differential Cross Section in the ERF

Derived from the kinematics

$$\frac{d\sigma_C}{d\epsilon_s d\Omega_s} = \frac{r_e^2}{2}\left(\frac{\epsilon_s}{\epsilon}\right)^2 \left(\frac{\epsilon_s}{\epsilon} + \frac{\epsilon}{\epsilon_s} - 1 + \cos^2\chi\right)\delta\left(\epsilon_s - \frac{\epsilon}{1+\epsilon(1-\cos\chi)}\right)$$

Total Cross Section in the ERF

Perform the integration.

$$\sigma_C(\epsilon) = \int_0^\infty d\epsilon_s \oint d\Omega_s \frac{d\sigma_C}{d\epsilon_s d\Omega_s}$$
$$= \frac{\pi r_e^2}{\epsilon^2}\left(4 + \frac{2\epsilon^2(1+\epsilon)}{(1+2\epsilon)^2} + \frac{\epsilon^2 - 2\epsilon - 2}{\epsilon}\ln(1+2\epsilon)\right)$$

Approximations

$$\sigma_C(\epsilon) \to \begin{cases} \sigma_T\left[1 - 2\epsilon + \frac{26}{5}\epsilon^2 + \mathcal{O}(\epsilon^3)\right] & \text{for } \epsilon \ll 1, \\ \frac{\pi r_e^2}{\epsilon}\left[\ln(2\epsilon) + 1/2 + \mathcal{O}(\epsilon^{-1})\right] & \text{for } \epsilon \gg 1. \end{cases}$$

Credit: Dermer & Menon (2009)

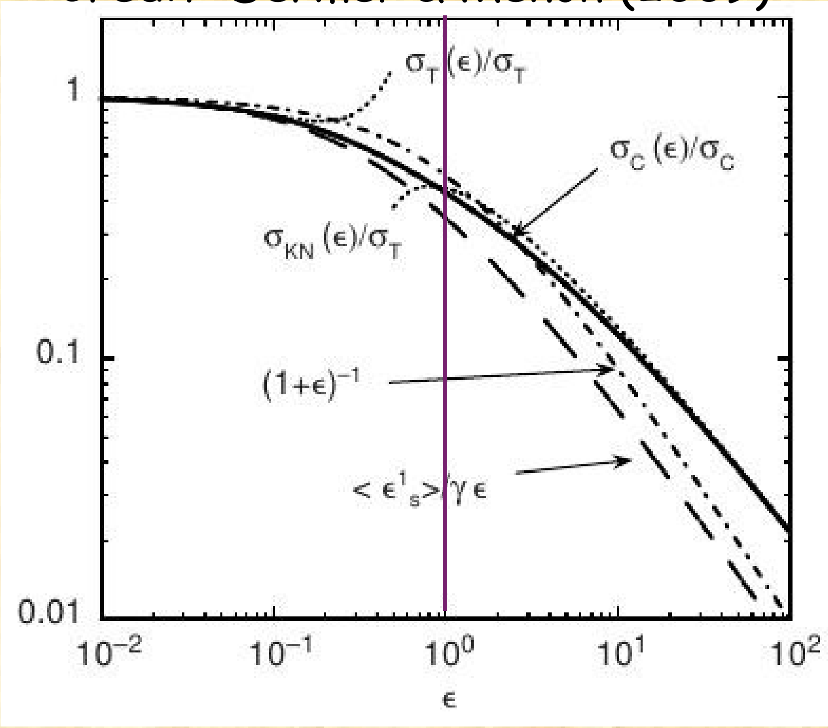

Inverse Compton Scattering - 3

Scattered emissivity in the LAB frame

$$j_C(\epsilon_s, \Omega_s) = m_e c^3 \epsilon_s \oint d\Omega \int_0^\infty d\epsilon \, n_{ph}(\epsilon, \Omega) \times \oint d\Omega_e \int_1^\infty d\gamma \, (1 - \beta_e \cos\psi) \, n_e(\gamma, \Omega_e) \frac{d\sigma_C(\bar{\epsilon})}{d\epsilon_s d\Omega_s}$$

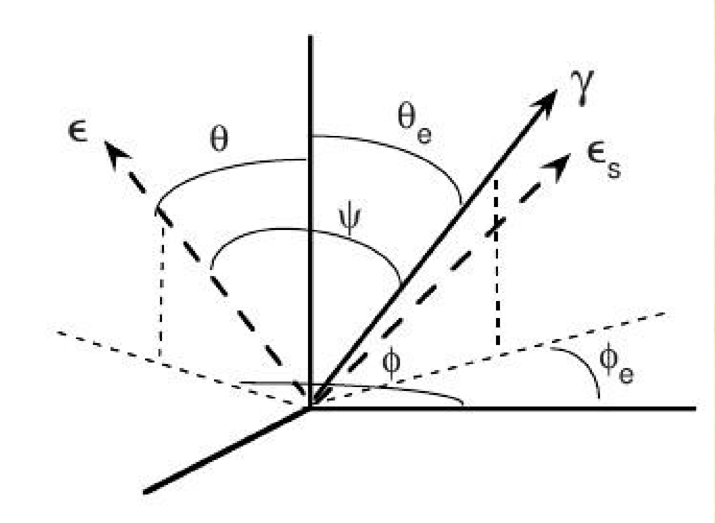

Credit: Dermer & Menon (2009)

How is the cross section in the ERF related to that in the Lab frame?

Inverse Compton power of a single electron (Thomson):

$$P_{compt} = \frac{dE_{rad}}{dt} = \frac{4}{3}\sigma_T c \gamma^2 \beta^2 U_{ph}.$$

Derivation based on Blumenthal & Gould (1970).

equivalently

$$P_{syn} = \frac{4}{3}\sigma_T c \, u_B \beta^2 \gamma^2$$

Energy loss timescale (Thomson):

$$t_{compt} = \frac{E}{P_{compt}} \propto U_{ph}^{-1} \gamma^{-1}$$

equivalently

$$t_{syn} = \frac{E}{P_{syn}} \propto U_B^{-1} \gamma^{-1}$$

Inverse Compton Scattering - 4

Scattered emissivity in the LAB frame

$$j_{\mathrm{C}}(\epsilon_s, \Omega_s) = m_e c^3 \epsilon_s \oint d\Omega \int_0^{\infty} d\epsilon\, n_{\mathrm{ph}}(\epsilon, \Omega) \times \oint d\Omega_e \int_1^{\infty} d\gamma\, (1 - \beta_e \cos\psi)\, n_e(\gamma, \Omega_e)\, \frac{d\sigma_{\mathrm{C}}(\bar{\epsilon})}{d\epsilon_s d\Omega_s}$$

Derive the Compton scattered emissivity for isotropic electron and photon distributions using the δ-function approximation for the cross section. The photon distribution is also monochromatic.

$$\frac{d\sigma_{\mathrm{T},\delta}}{d\epsilon_s d\Omega_s} \cong \sigma_{\mathrm{T}} \delta(\Omega_s - \Omega_e) \delta(\epsilon_s - \gamma\bar{\epsilon}) H(1 - \bar{\epsilon}).$$

Answer:

$$\epsilon_s j_{\mathrm{T},\delta}(\epsilon_s) = \frac{1}{2} c \sigma_{\mathrm{T}} u_0 \left(\frac{\epsilon_s}{\epsilon}\right)^3 \int_{\max(\epsilon_s, \sqrt{\epsilon_s/2\epsilon})}^{\infty} d\gamma\, \frac{n_e(\gamma)}{\gamma^4}$$

Inverse Compton Scattering - 5

With δ-function approximation

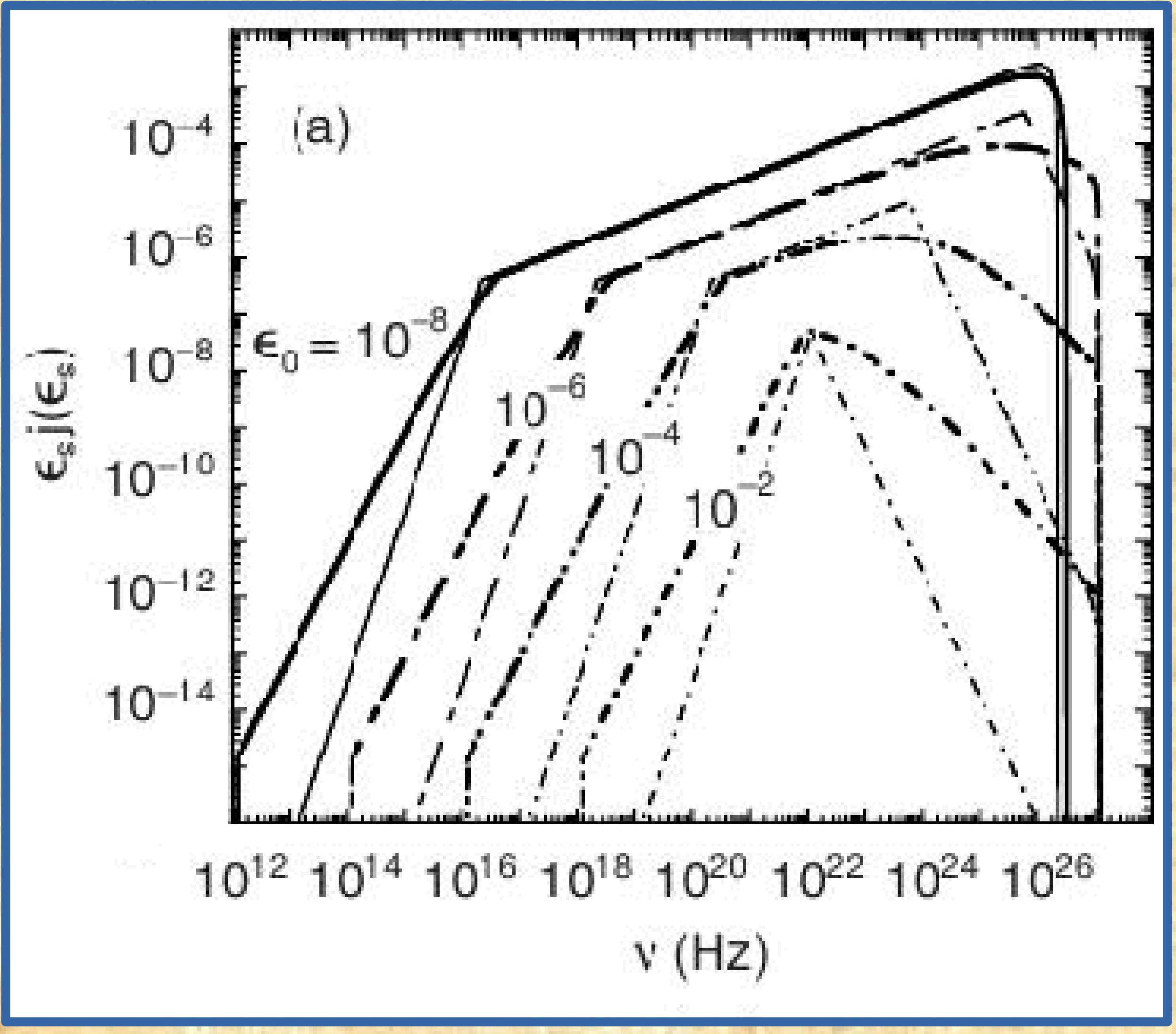

The approximation breaks down as the photon energy increases....

Credit: Dermer & Menon (2009)

Models for blazar emission

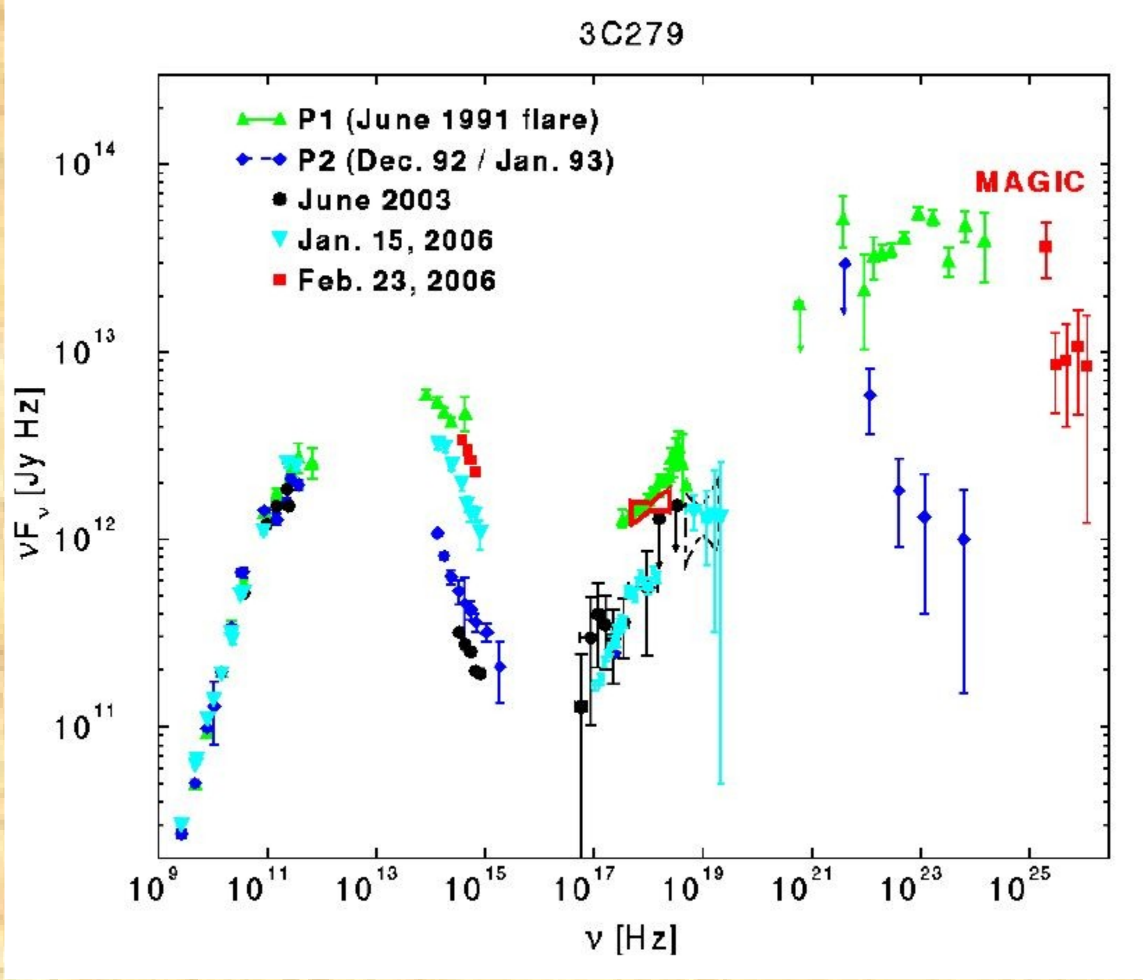

-4/4-

Leptonic models

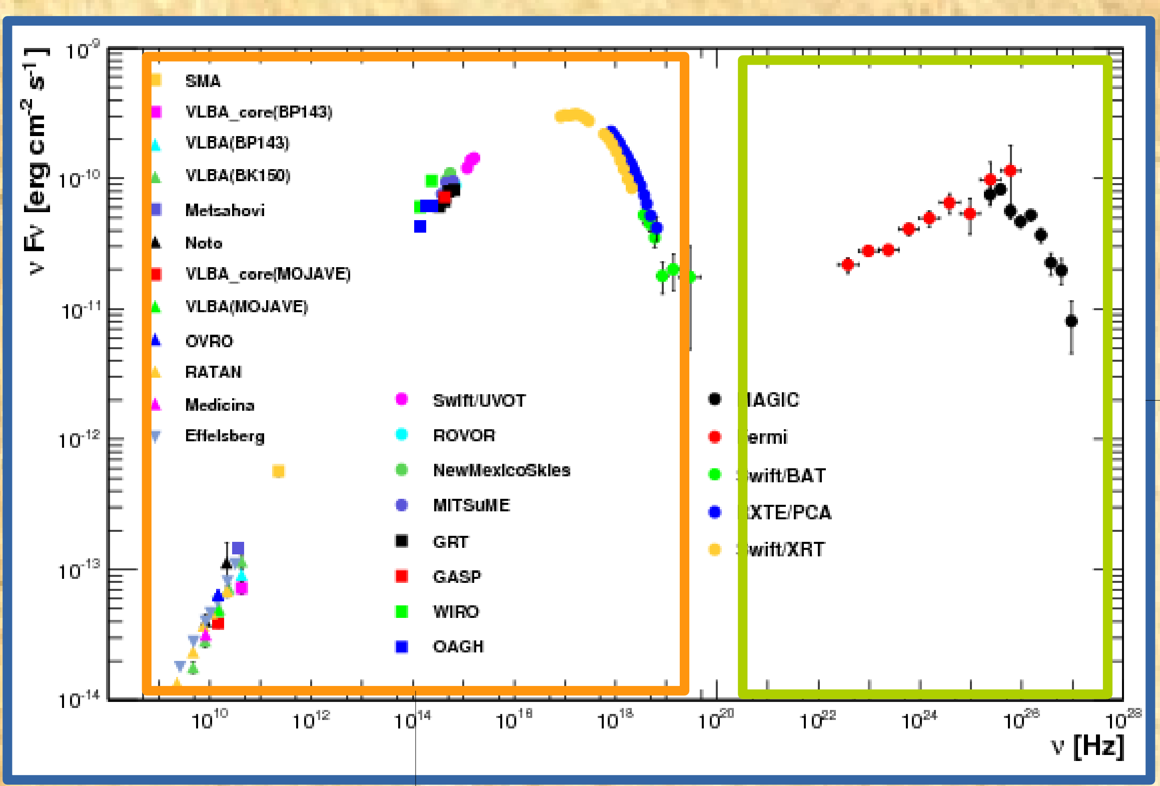

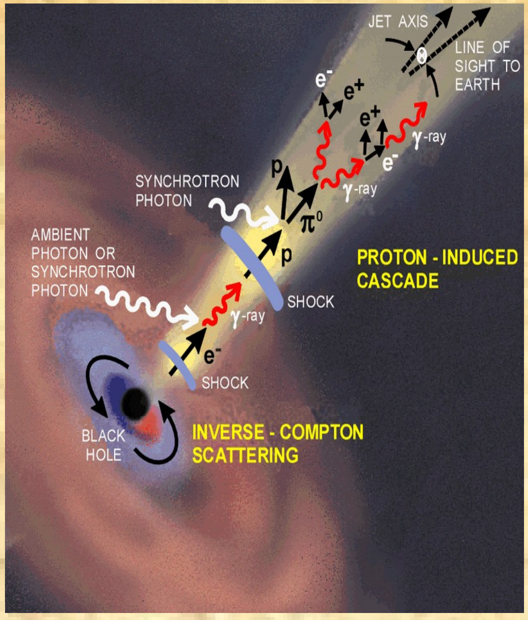

Inverse Compton scattering of synchrotron photons (SSC) or of external photons (ECS) by relativistic electrons

Synchrotron radiation from relativistic electrons in the source

Early bibliography: *Maraschi et al. 1992, Sikora et al. 1994, Dermer & Schlickeiser 1994, Mastichiadis & Kirk 1995, Bloom & Marscher 1996, Rieger et al. 1998*

Hadronic models

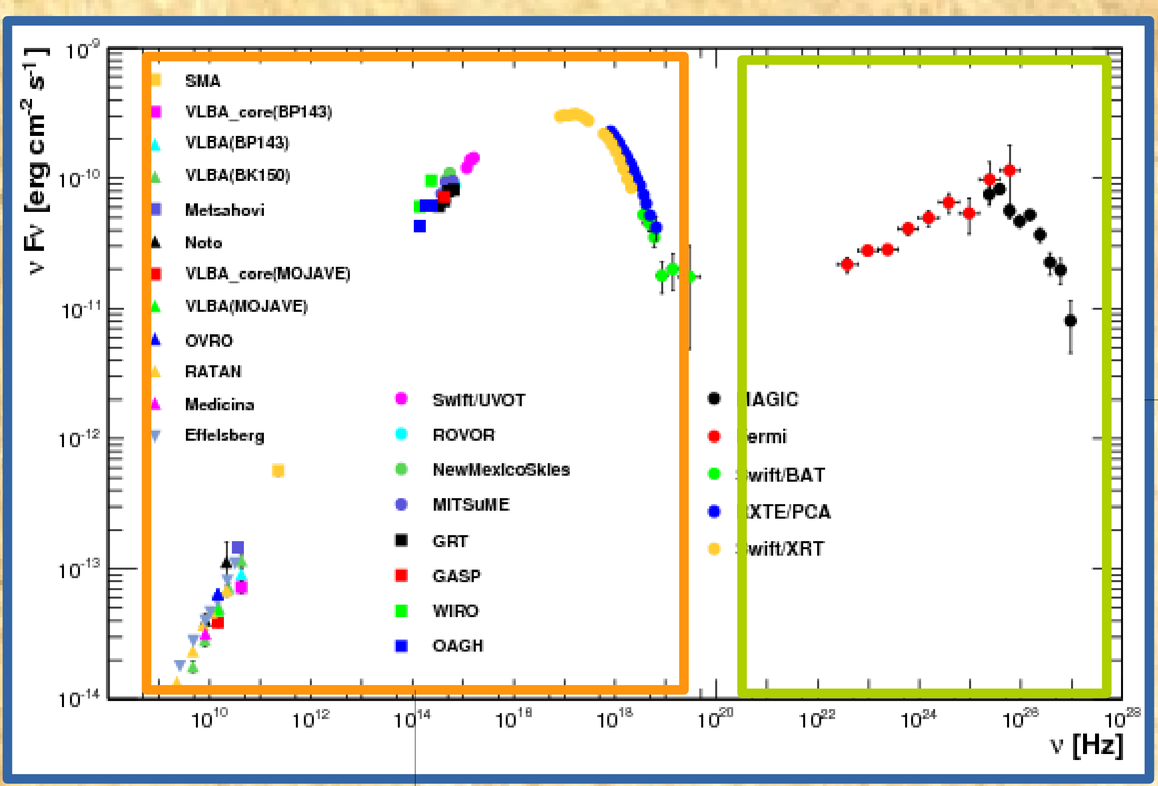

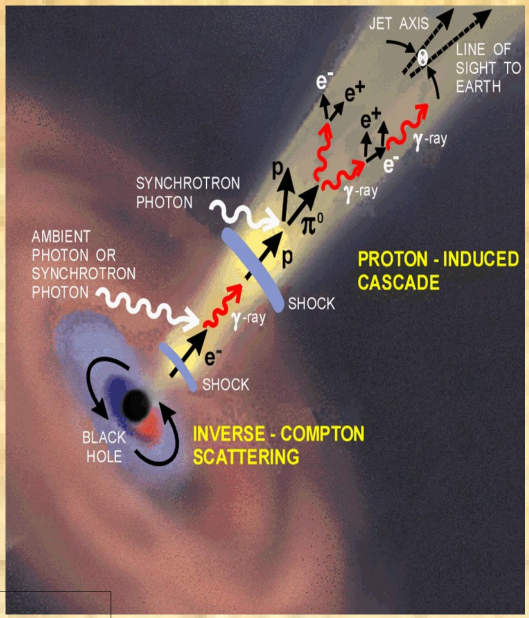

- Synchrotron radiation from relativistic protons

Synchrotron radiation from relativistic electrons in the source

- Synchrotron radiation from relativistic electrons produced by photohadronic processes

- γ-rays from pion decays

Bibliography: *Mannheim & Biermann 1992, Aharonian 2000, Atoyan & Dermer 2001, Muecke et al. 2003, Mastichiadis et al. 2013, Boettcher et al. 2013*

How do one-zone models work?

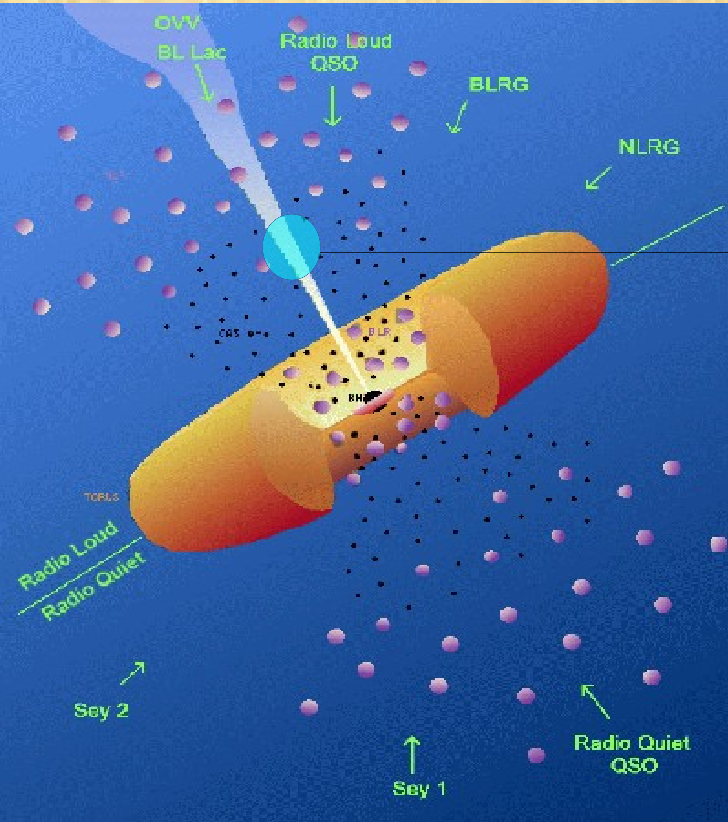

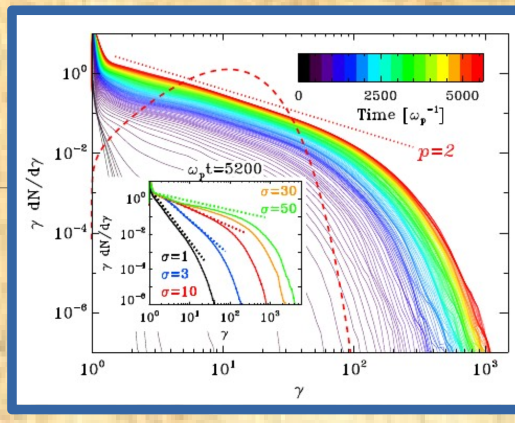

Injection of Particles (Q_e)

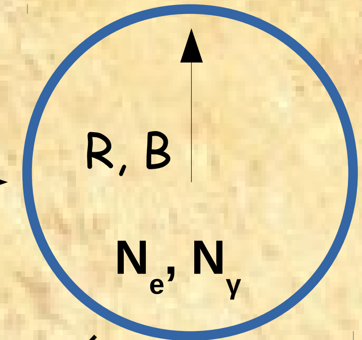

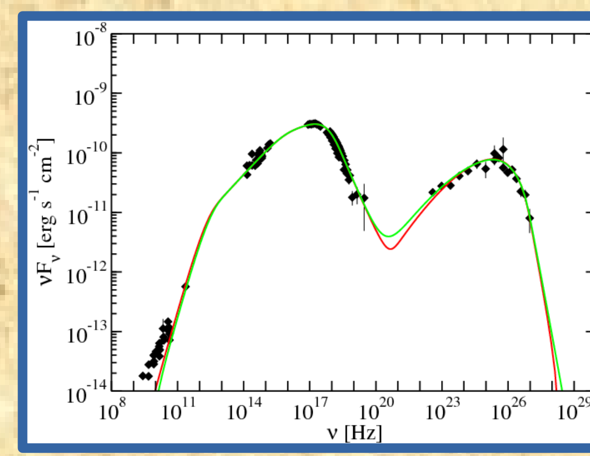

Observed Emission (N_γ ; Γ, θ)

$$\frac{\partial N_e(\gamma,t)}{\partial t}+Q_e(\gamma,t;N_e,N_\gamma)+L_e(\gamma,t;N_e,N_\gamma)=0$$

$$\frac{\partial N_\gamma(\varepsilon,t)}{\partial t}+Q_\gamma(\varepsilon,t;N_e,N_\gamma)+L_\gamma(\varepsilon,t;N_e,N_\gamma)=0$$

Synchrotron Self-Compton (SSC)

- Electrons produce synchrotron photons
- Electrons up-scatter the synchrotron photons to higher energies
- Synchrotron radiation depends on N_e
- Inverse Compton scattered radiation depends on N_e
- If electrons lose energy not by synchrotron but by SSC photons → higher order Compton scatterings → more severe energy losses of electrons → higher SSC radiation → Compton Catastrophe

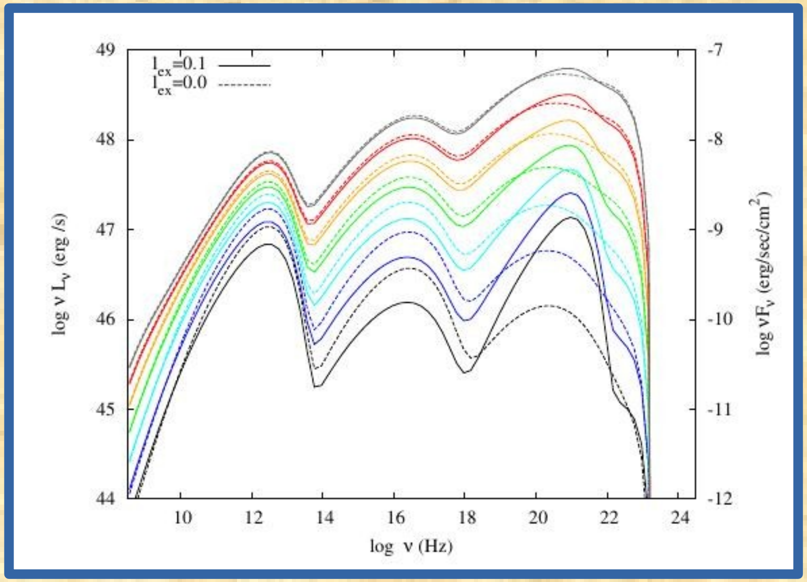

Petropoulou, Piran & Mastichiadis, 2015, MNRAS

External Compton model (ECS)

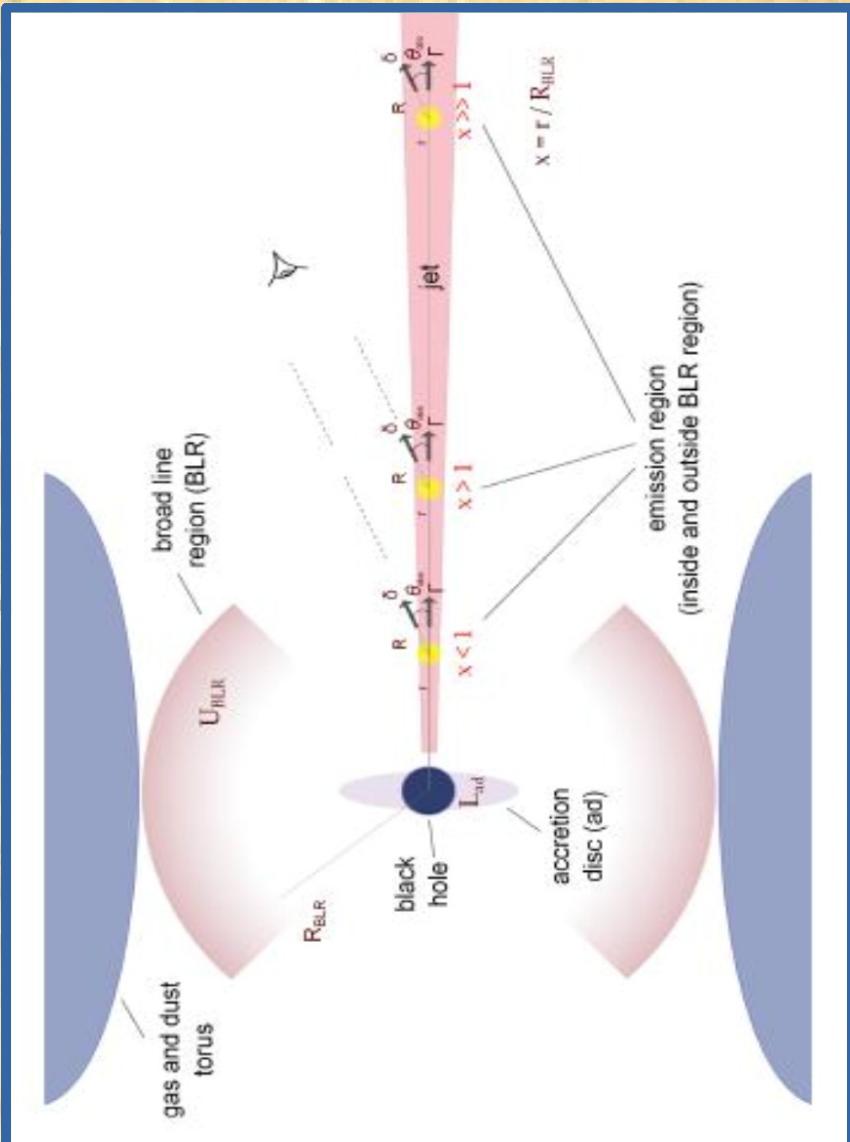

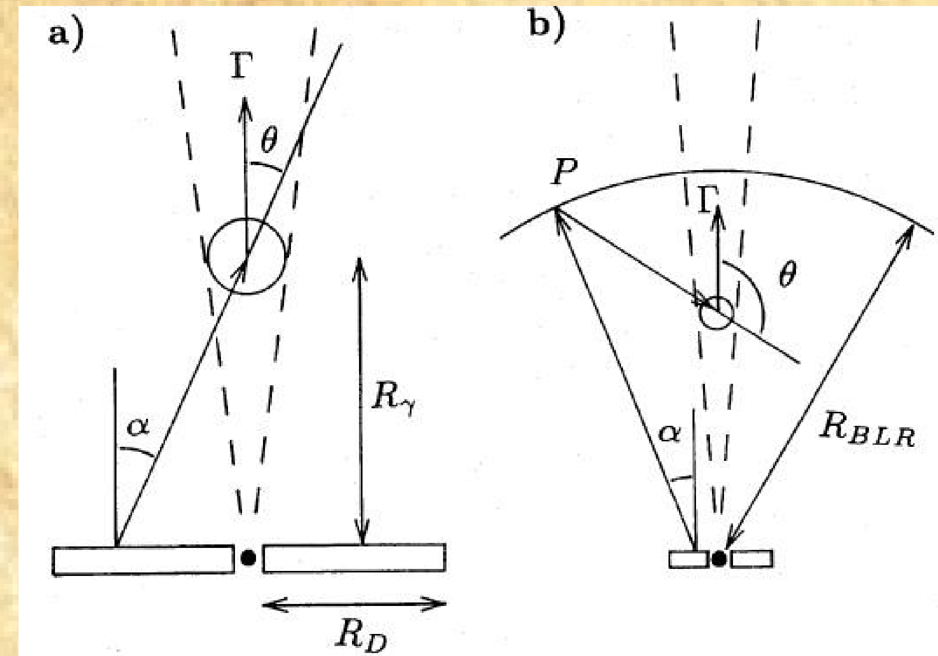

Accretion disk ~ illumination from "behind"

BLR ~ Isotropic photon field

Early bibliography: *Dermer, Schlickeiser, Mastichiadis 1992, Dermer & Schlickeiser 1993, Dermer 1995, Ghisellini & Madau 1996*

ECS: useful relations

External photon energy density: $$u'_0 \approx \frac{4}{3}\Gamma^2 u_0$$

External photon energy: $$\varepsilon'_0 \approx \Gamma \varepsilon_0$$

Peak energy of EC component: $$\varepsilon_{IC} \approx \frac{4}{3}\Gamma \delta \gamma^2 \varepsilon_0$$

Ratio of peak luminosities: $$\frac{L_{EC}}{L_{syn}} \approx \frac{u'_0}{u'_B} \approx \frac{\Gamma^2 u_0}{u'_B}$$

$$\frac{L_{EC}}{L_{syn}} \approx \frac{9}{2}\frac{u_0}{B_{cr}^2}\left(\frac{\varepsilon_{IC}}{\varepsilon_s}\right)^2\left(\frac{m_e c^2}{\varepsilon_0}\right)^2$$

One-zone SSC model

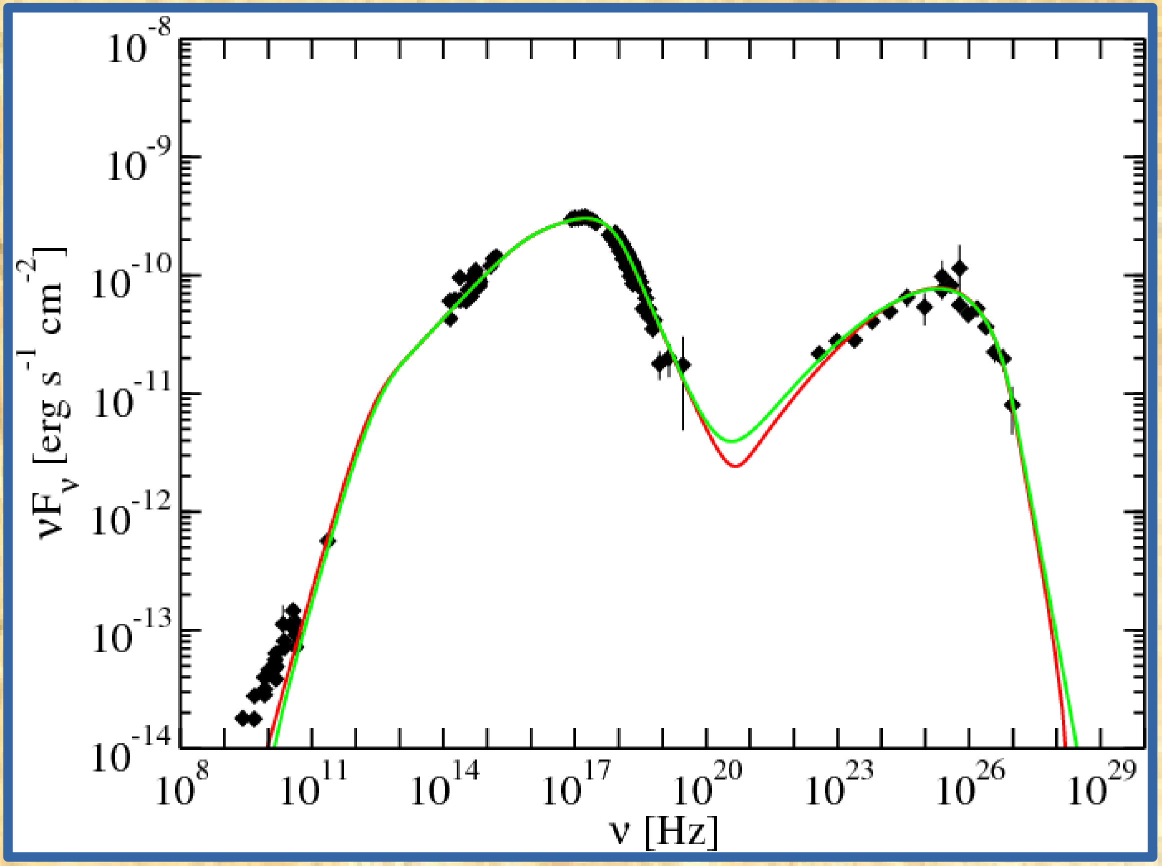

For the derivation see Mastichiadis & Kirk, 1997, A&A

See also Ghisellini et al. 1996, Tavecchio et al. 1998

7 observables and 7 parameters → estimates of:
- the Doppler factor,
- the size of the source
- the magnetic field, and
- the specifics of relativistic electrons (high energy cut-off, spectral index)

One-zone SSC model

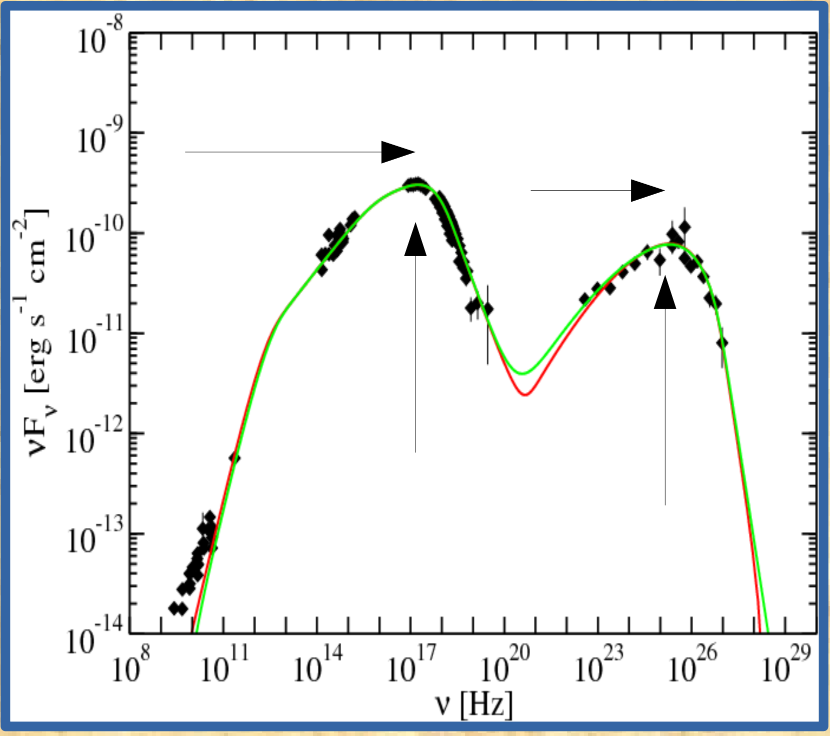

Variability timescale: $R \leq c\delta\Delta t_v$

Peak synchrotron energy: $\varepsilon_s = \delta b \gamma^2 m_e c^2$

Peak IC energy (Thomson): $\varepsilon_{IC} = \frac{4}{3}\delta \gamma^2 \varepsilon_s$

Ratio of peak luminosities:

$$\frac{L_{SSC}}{L_s} = \frac{u_s}{u_B} = \frac{L_s}{4\pi c R^2 \delta^4 u_B}$$

Maria Petropoulou (Purdue) & Stavros Dimitrakoudis (UofA)

Blazar SED modeling

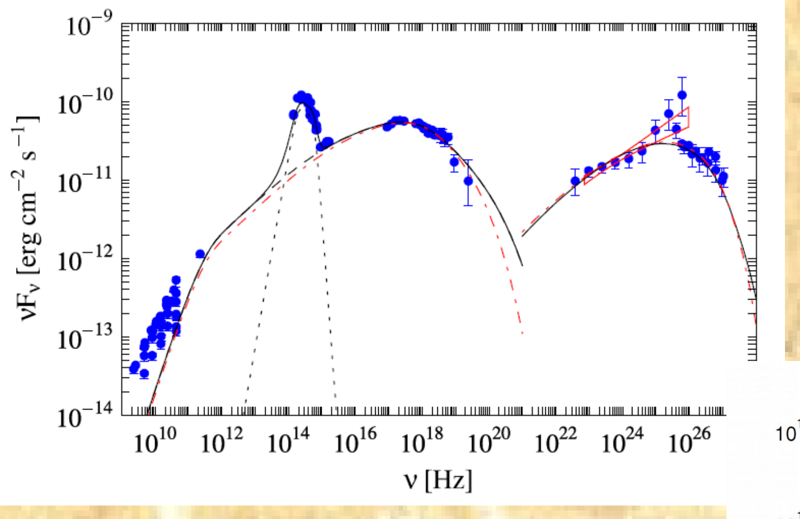

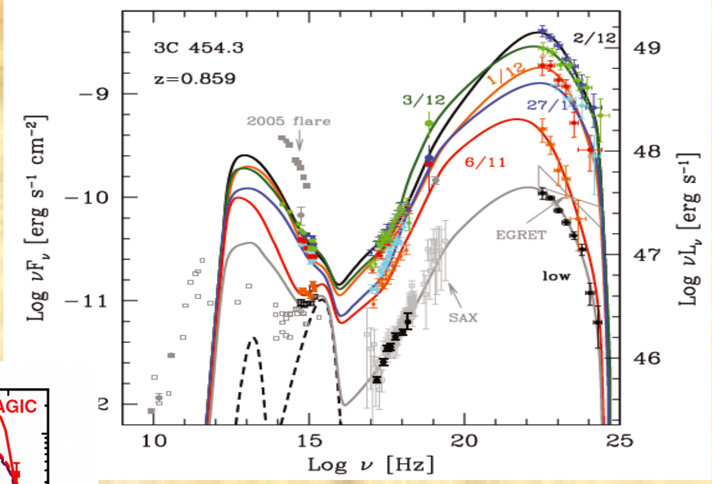

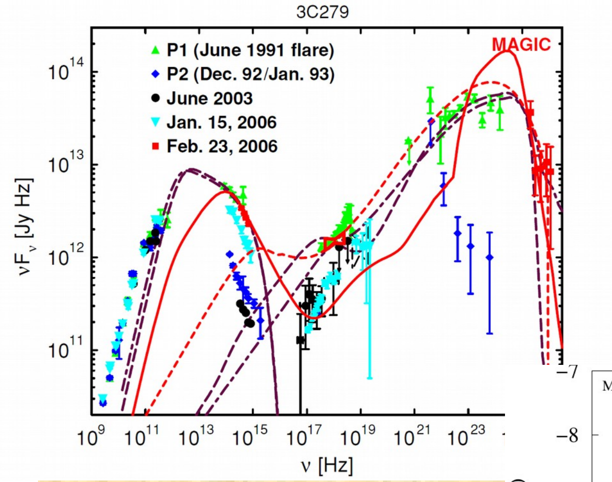

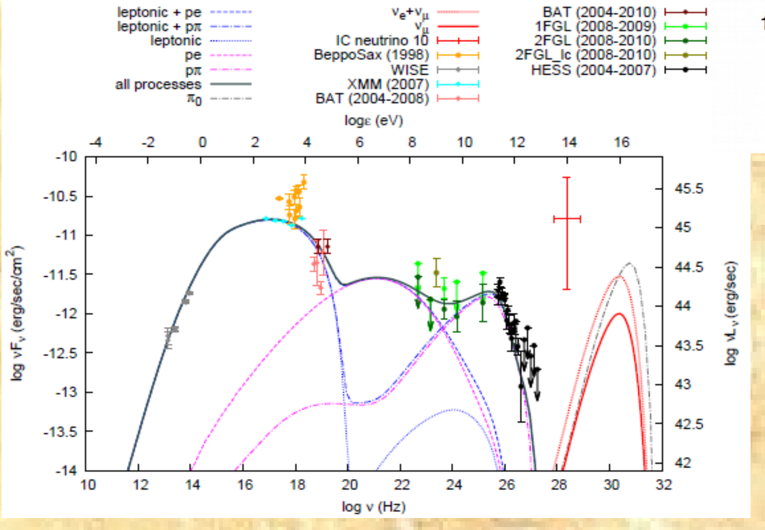

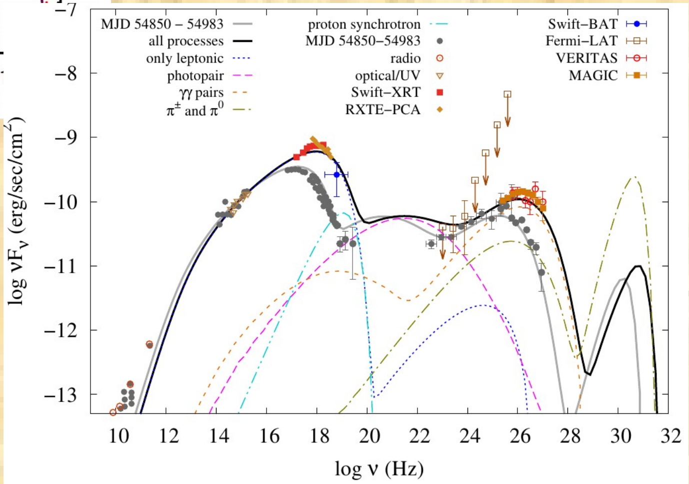

Blazar SED modeling

Based on the numerical code by A. Tramacere et al 2009, A&A, 501, 879 (htpp://.isdc.unige.ch/sedtool/)

- Source and jet parameters: R=1e16 cm, B=0.1 G, Γ_j=10, θ=3.5 deg
- Electron distribution parameters: γ_{min} = 10, γ_{max}=1e5, p=2

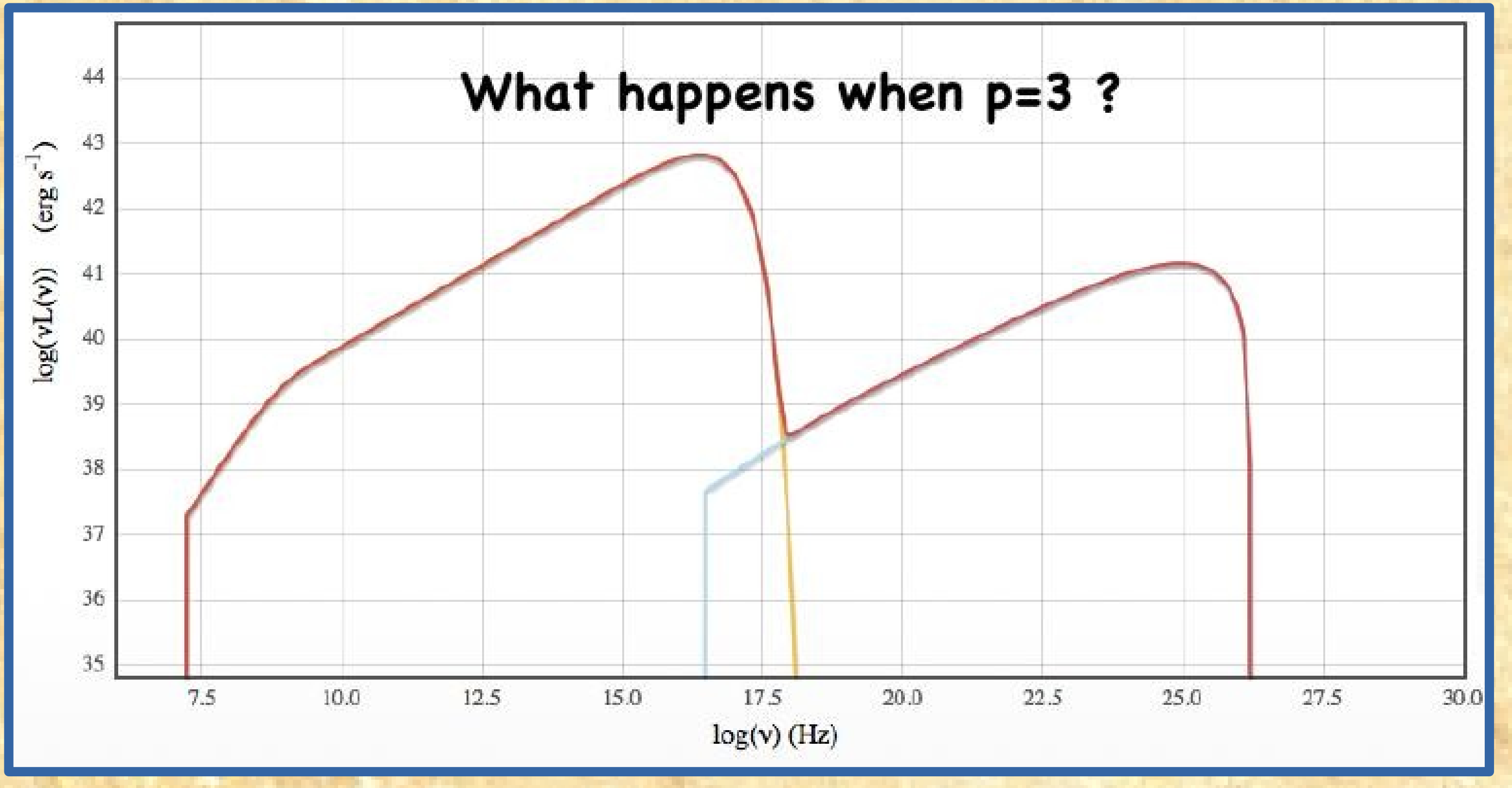

Blazar SED modeling

Based on the numerical code by A. Tramacere et al 2009, A&A, 501, 879 (htpp://.isdc.unige.ch/sedtool/)

- Source and jet parameters: R=1e16 cm, B=0.1 G, Γ_j=10, θ=3.5 deg
- Electron distribution parameters: γ_{min} = 10, γ_{max}=1e5, p=3

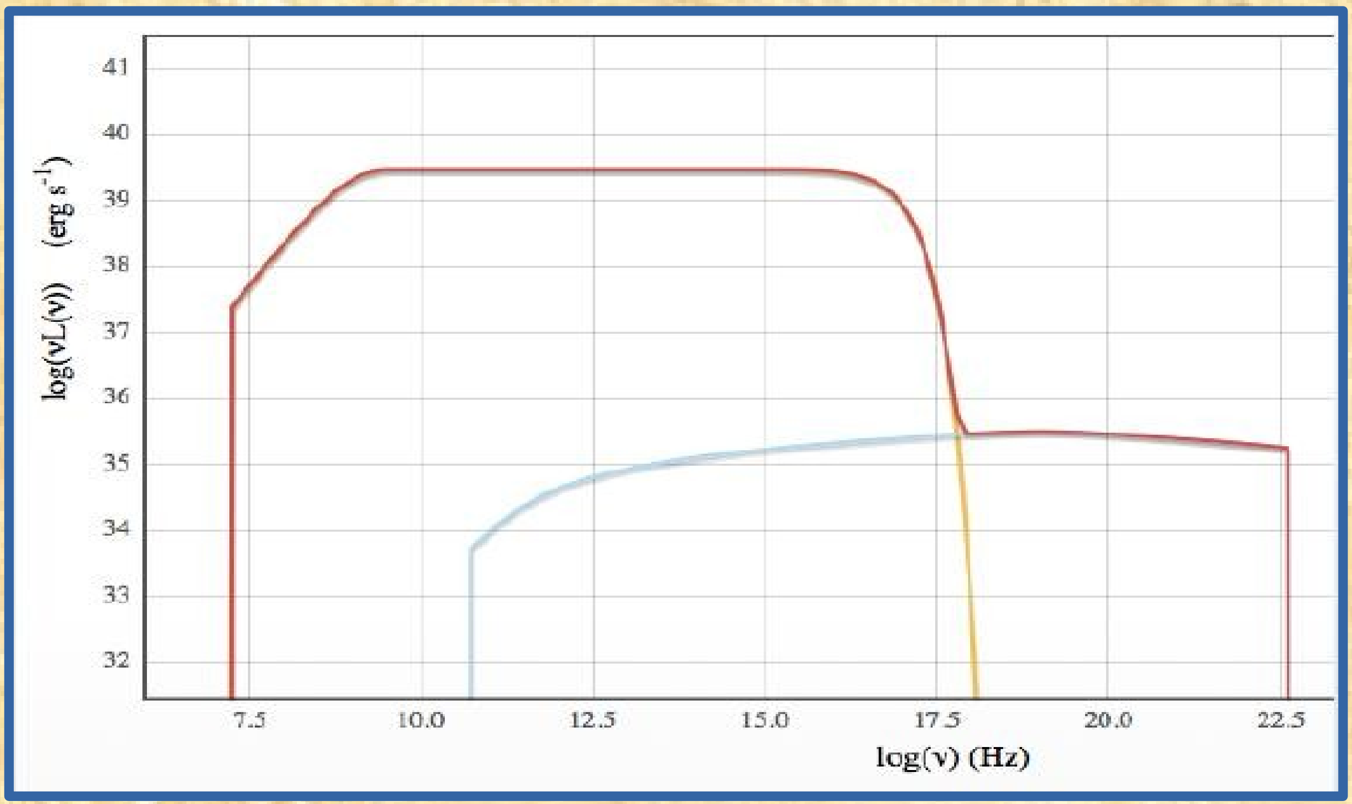

Blazar SED modeling

Based on the numerical code by A. Tramacere et al 2009, A&A, 501, 879 (htpp://.isdc.unige.ch/sedtool/)

- Source and jet parameters: R=1e16 cm, B=0.1 G, Γ_j=10, θ=3.5 deg
- Electron distribution parameters: γ_{min} = 10, γ_{max}=1e5, p=2

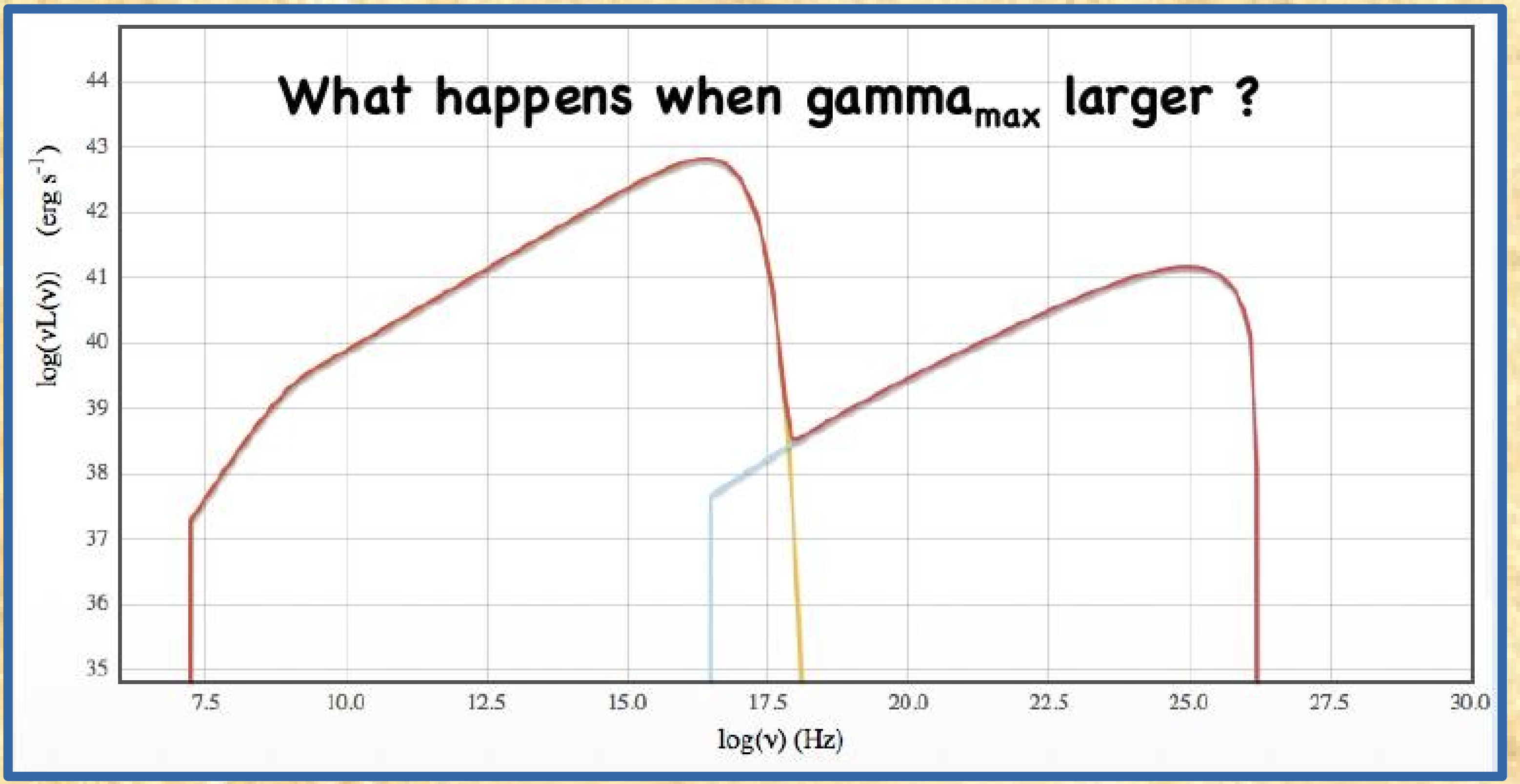

Blazar SED modeling

Based on the numerical code by A. Tramacere et al 2009, A&A, 501, 879 (htpp://.isdc.unige.ch/sedtool/)

- Source and jet parameters: R=1e16 cm, B=0.1 G, Γ_j=10, θ=3.5 deg
- Electron distribution parameters: γ_{min} = 10, γ_{max}=1e6, p=2

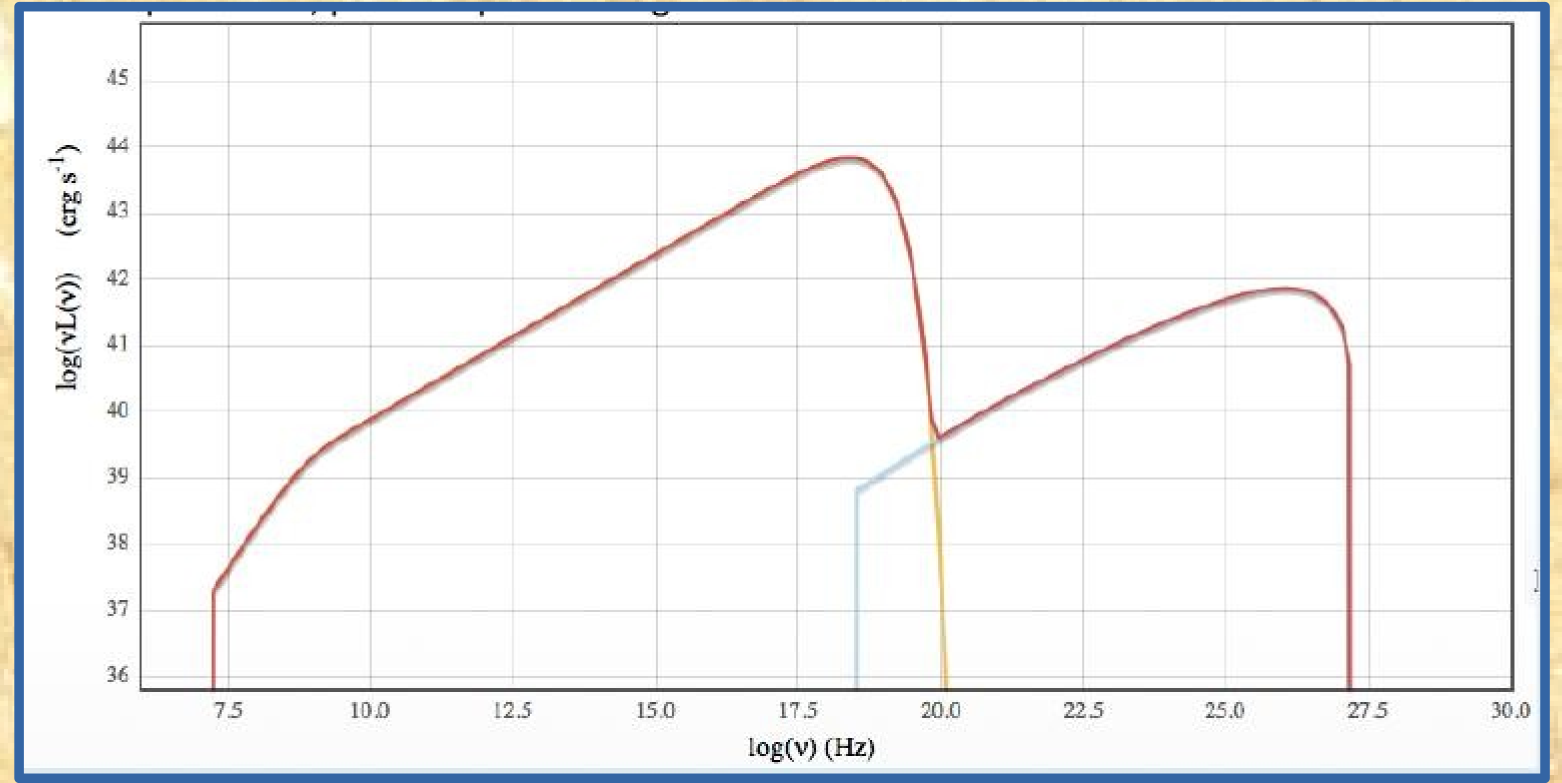

Blazar SED modeling

Based on the numerical code by A. Tramacere et al 2009, A&A, 501, 879 (htpp://.isdc.unige.ch/sedtool/)

- Source and jet parameters: R=1e16 cm, B=0.1 G, Γ_j=10, θ=3.5 deg
- Electron distribution parameters: γ_{min} = 10, γ_{max}=1e5, p=2

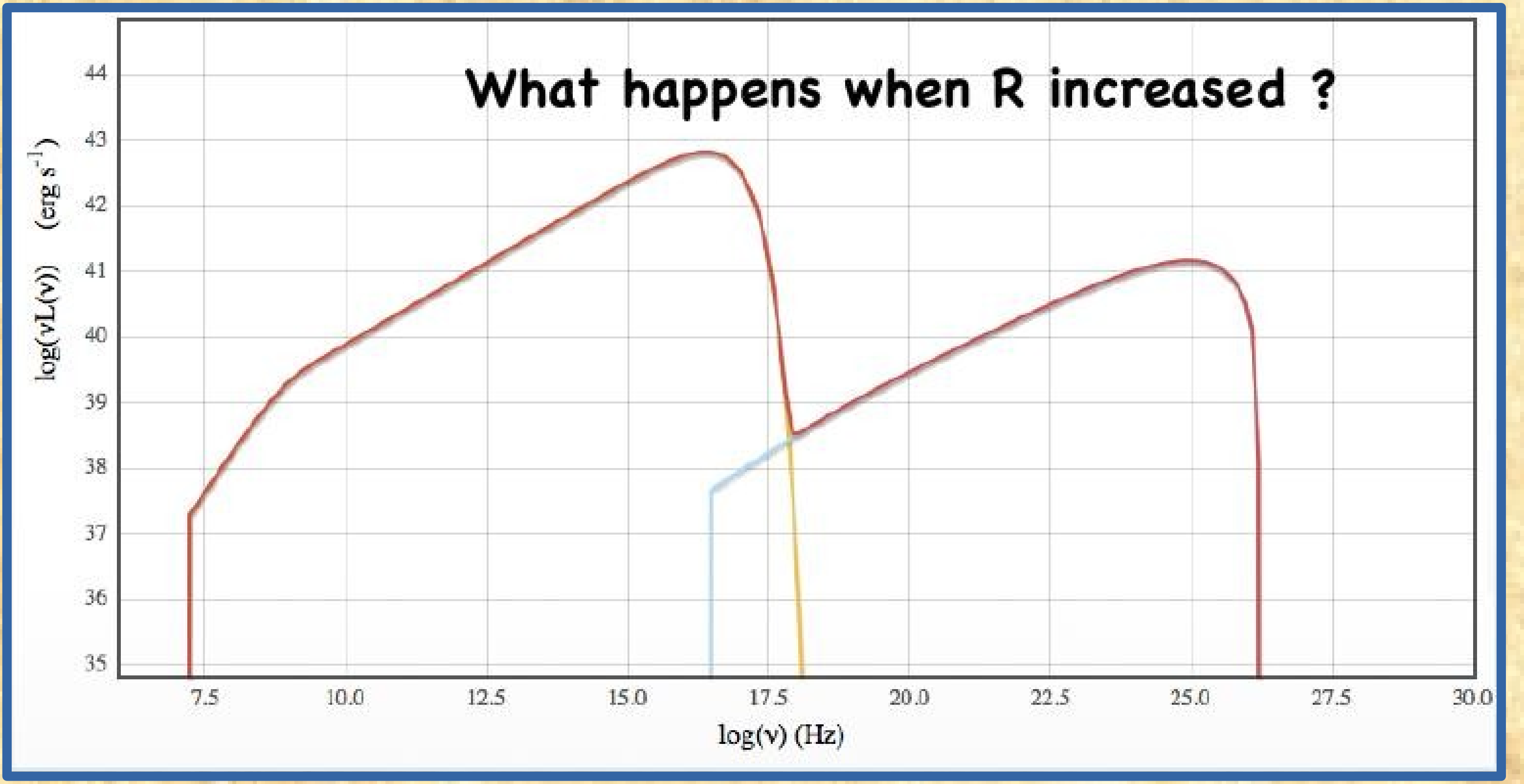

Blazar SED modeling

Based on the numerical code by A. Tramacere et al 2009, A&A, 501, 879 (htpp://.isdc.unige.ch/sedtool/)

- Source and jet parameters: R=1e17 cm, B=0.1 G, Γ_j=10, θ=3.5 deg
- Electron distribution parameters: γ_{min} = 10, γ_{max}=1e5, p=2

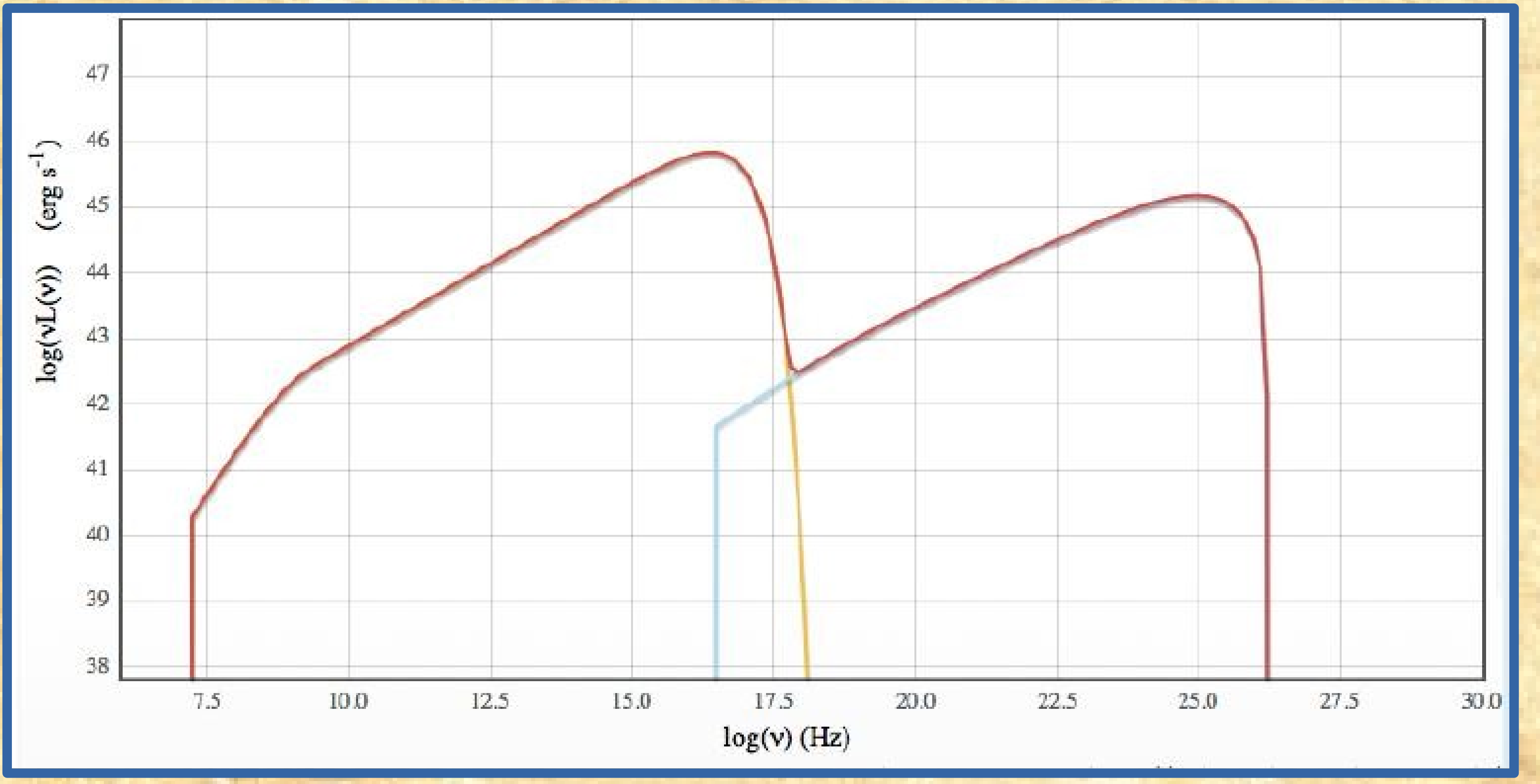

Blazar SED modeling

Based on the numerical code by A. Tramacere et al 2009, A&A, 501, 879 (htpp://.isdc.unige.ch/sedtool/)

- Source and jet parameters: R=1e16 cm, B=0.1 G, Γ_j=10, θ=3.5 deg
- Electron distribution parameters: γ_{min} = 10, γ_{max}=1e5, p=2

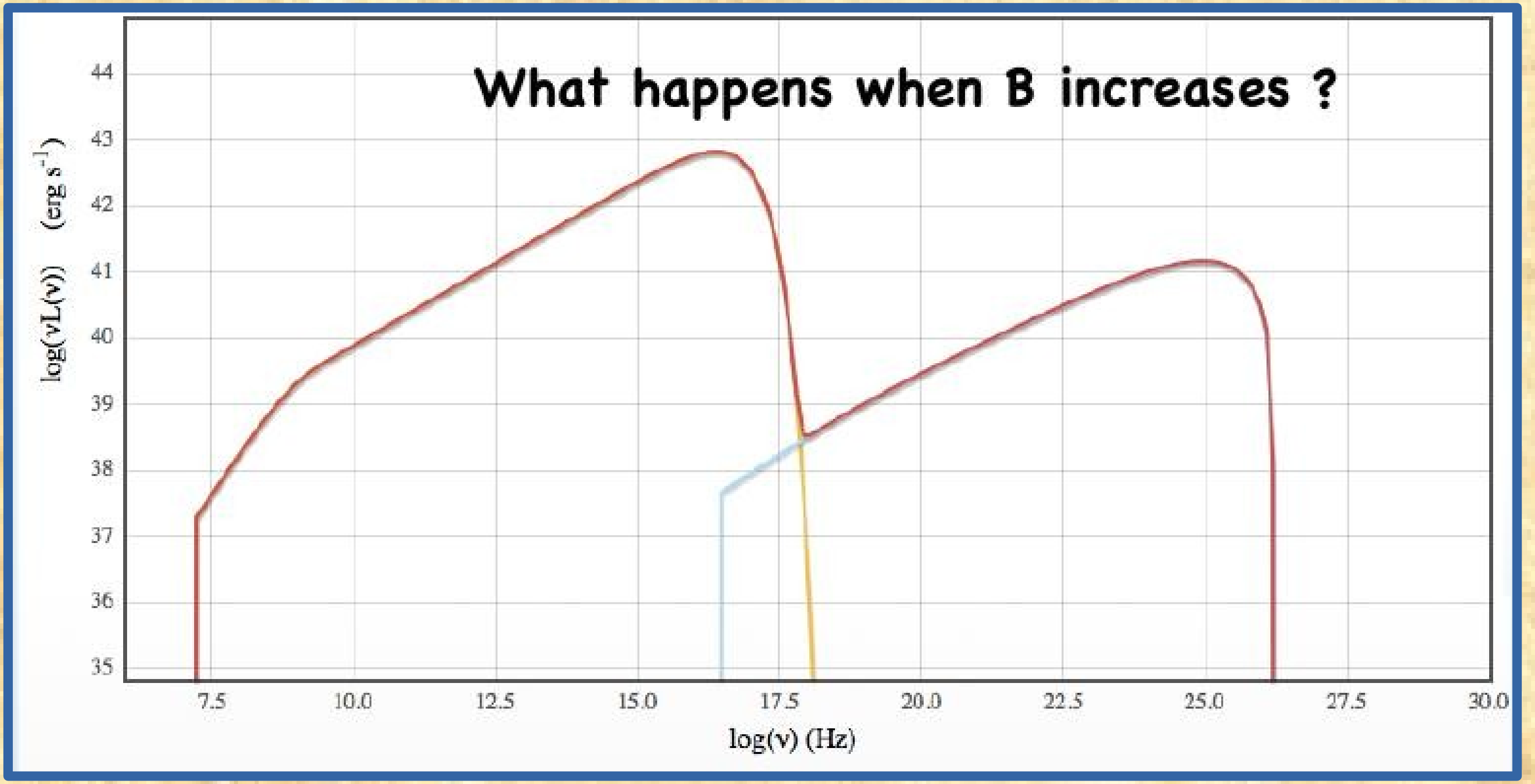

Blazar SED modeling

Based on the numerical code by A. Tramacere et al 2009, A&A, 501, 879 (htpp://.isdc.unige.ch/sedtool/)

- Source and jet parameters: R=1e16 cm, B=1 G, Γ_j=10, θ=3.5 deg
- Electron distribution parameters: γ_{min} = 10, γ_{max}=1e5, p=2